# Development of a Process Simulation Model of a Pultrusion Line

Miro Duhovic, Pravin Aswale, Dominic Schommer, Joachim Hausmann

Institut für Verbundwerkstoffe GmbH, Erwin-Schrödinger-Str., Gebäude 58, 67663 Kaiserslautern, Germany

## 1 Introduction

The applications for fiber reinforced plastic (FRP) composite structures have increased tremendously in the automotive and aerospace industries due to their lightweight nature. However, because of their high manufacturing cost, composite structures are typically only used for high-end parts. The reason behind this is the relatively low mass production rate of composite structures. Among the various composite manufacturing methods available, pultrusion is a continuous production process, meaning that the potential for mass production is there, if the process can be made fast enough. The process of pultrusion is defined as extrusion with pulling, in contrast with the conventional 'extrusion process', which is used for manufacturing uniform cross section structures such as circular bars, hollow tubes, I section beams etc. [1] [2]. Currently, pultrusion has a wide range of applications in the "architecture, transportation, construction, agriculture, chemical engineering, aircraft, and aerospace industry" [2]. On the basis of the polymer used in the manufacturing process, pultrusion can be divided into two types namely: thermoset and thermoplastic pultrusion. Many studies in the past have been conducted on thermoset pultrusion whose main advantage over thermoplastic pultrusion is the fiber impregnation, or 'wetting out of the fiber reinforcement' due to the resin's low viscosity [3]. On the other hand, thermoplastic pultrusion can create parts which are recyclable, post formable, weldable, have excellent environmental stability and good mechanical properties such as high "fracture toughness, higher damage resistance" [1]. Due to such economic, environmental and mechanical advantages, many researchers have contributed to the development of thermoplastic pultrusion mainly in the field of fiber impregnation with thermoplastic resins [1] [4] [5]. With the advancement in thermoplastic prepreg technologies, pultrusion experiments with pre-consolidated tapes (PCT), powder coated tow-pregs and commingled yarns were performed and studied [1]. Moreover, in the early 1990s, thermoplastic pultrusion models were developed by researchers in order to understand the workings of the process [3] [6]. Most of the current research is focused mainly on investigating the effects of process and material parameters on the mechanical performance of the pultruded part. However, the interrelationship between the materials, process, and product is still not fully understood or has been incorporated into a complete CAE processing chain. The development of analytic, computational, and experimental approaches continues and the need of a fully developed simulation model, which can be used to optimize process parameters, avoid a trial and error approach and to improve productivity still exists.

In recent years with the advancement in computational capability, new numerical simulation techniques have been developed. The important goal of the numerical simulation is to build a virtual model of the physical environment, where the approximation and simplification of reality plays a very important role. The thermoplastic pultrusion process is a complex process, containing solid (die and fibers) and fluid (polymer) parts. Furthermore, during the processing of the fiber reinforced thermoplastic, due to the heat transfer from the die segments, the polymer undergoes changes from a solid to liquid phase and back again. To build a numerical simulation model, not only a thorough understanding of the physical situation is required, but also the possibilities with respect to the available simulation methods. The governing equations of the pultrusion process require both solid mechanics and fluid dynamics concepts to obtain a numerical solution. The development of multiphysics problem-solving Fluid-Structure Interaction (FSI) capabilities in general FEA software codes over the past few years can be used to solve such governing equations. Nowadays, methods including the Discrete Element Method (DEM) and Smoothed Particles Hydrodynamics (SPH) have already been used to solve FSI problems. Another method is the Arbitrary Lagrangian-Eulerian (ALE) approach, which is formulated by combining advantages of both the Lagrangian and Eulerian approaches [7] [8].

This paper presents the development of a pultrusion line process simulation model using the ALE/FSI capabilities available in LS-DYNA. A study of the parameters involved in the pultrusion process and the mechanics behind them is an important goal of the work. Processing parameters such as temperature, pressure, die geometry, pulling speed are studied with the help of thermal, impregnation and pressure models found in the literature. On the basis of this research and real world input data provided by an industry partner, the setup of an actual pultrusion line process simulation model has been developed. Different models are tested in order to optimize the simulation model giving the desired output at the base pulling speed (0.2 m/min). After the successful development of the simulation model, a parameter study investigating the effect of higher pulling speed and variation in input material volume on temperature and pressure in various sections of the die is carried out.

## 2 Sate of the art

### 2.1 Thermoplastic pultrusion

Pultrusion using fiber reinforced thermoplastic (FRP) as a raw material is called thermoplastic pultrusion. The matrix can be thermoplastic resins such as polypropylene (PP), polyamide (PA), polybutylene terephthalate (PBT) and even aerospace grade thermoplastic polymers such as polyether ether ketone (PEEK). A schematic of the process is shown in Figure 1. The input material for thermoplastic pultrusion can be fiber reinforcements of different types (glass, carbon, etc.) and forms such as continuous rovings, woven mat fabric reinforcement, a braided structure or already consolidated continuous fiber reinforced prepregs [2]. Combining the reinforcement fibers with the resins can therefore be done before the preheating process (on the same production line) or by using direct prepregs (prepregs manufactured separately and used for other manufacturing processes) such as preconsolidated tapes [2] [5]. Before entering the preheating stage, fibers and polymer matrix are passed through a guiding system, which is designed based on the required output profile. In the preheater, the composite material is heated to a temperature below the melting point of the polymer matrix and is then fed into the heated pressurization and consolidation die [9]. The fiber reinforcements are impregnated (if not already) here with the melted matrix and the pultruded composite structure is formed [6]. In the heated die, the pressure, temperature and the die geometry play important roles in determining the final mechanical properties of the pultruded composite structure [9]. The composite material is continuously pulled by the haul-off equipment at the pulling force required to overcome the resistance in the die [6]. In addition, between the pulling system and the heated die, a cooling die is provided to help with the solidification of the material [3]. Finally, the pultruded structure is cut as per the required length by a cutter.

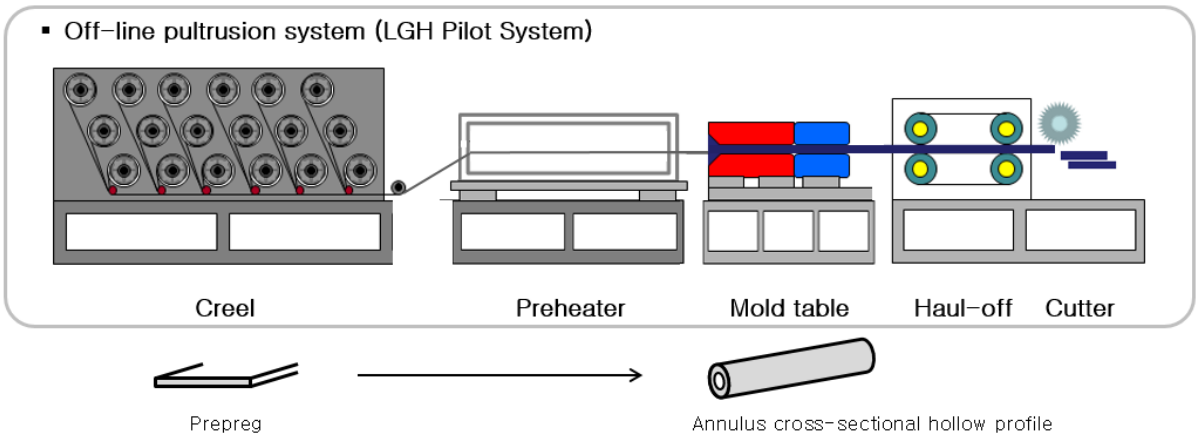


*Fig.1: Schematic diagram of a LGH thermoplastic prepreg based pultrusion line [2]*

The nature of the parameters such as, the temperature of the preheater and die, pressure on the material, die geometry, pulling speed have been described in the subsequent sections and are based on real-world equipment. Impregnation methods as well as the degree of impregnation (DOI) based on the aforementioned parameters have been left out, as this is not considered in the current simulation model.

# 3 Model preparation

## 3.1 Input data

"Real-world" input data required for the set-up of a realistic process simulation model has been provided by LG Technology Center Europe and LG Hausys South Korea. The pultrusion process set-up and tooling is shown in Figures 1, 2 and 3. A mandrel is placed in the center of the die and is connected to one leg of the die. The initial and final outer diameter of the die is 80 mm and 20 mm respectively. The die is divided into 6 segments each with an equal length of 230 mm, where the first four segments are hot and remaining last two segments are cold. The outer diameter is reduced from 80 mm to 20 mm gradually over each segment and remains constant in the last two segments as shown in Figure 2.

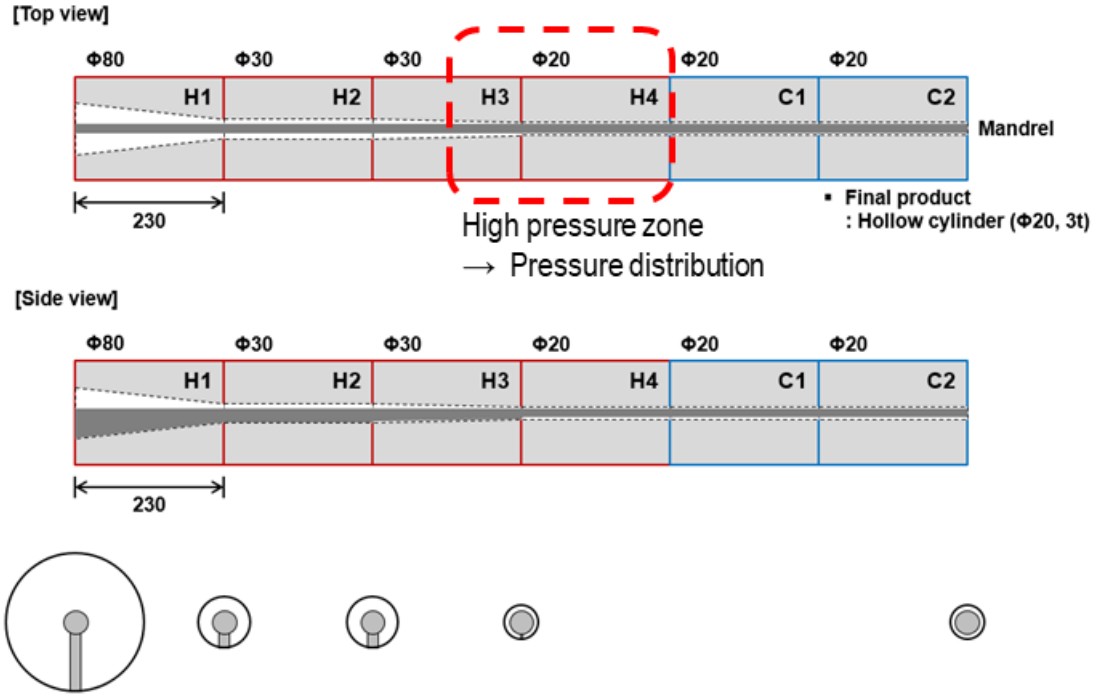


*Fig.2: Details of die tooling and mandrel configuration*

The hot die segments (H1 to H4) are heated to a temperature of 240°C by using 700 W heaters, whereas the cold die segments C1 and C2 are maintained at room temperature (27°C). The input material for the pultrusion is a unidirectional glass fiber polyamide 6 (GF/PA6) thermoplastic prepreg. The material is supplied in the form of three prepreg sheets which pass through a trajectory guide as shown in Figure 3, (left and middle), before entering the first heating die. During the preheating stage, the prepreg material is heated to a temperature of 150°C via a preheating unit set to a temperature of 220°C. The thickness of the spider-leg (in mm), which supports the mandrel and connects the mandrel to the die, is shown in Figure 3 (right) and is present only in the first 3 segments of the die.

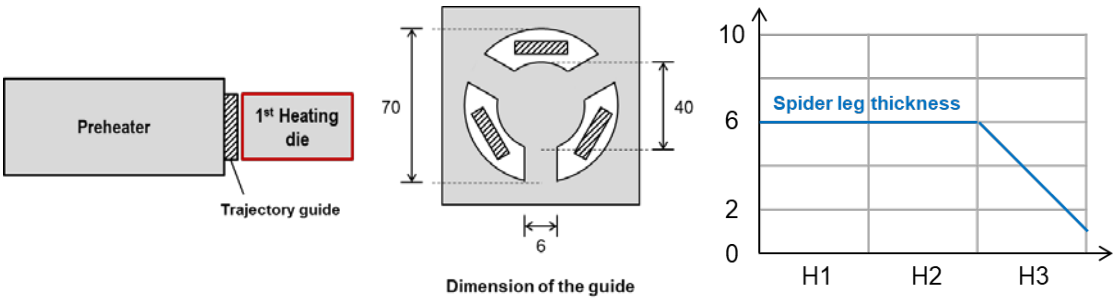


*Fig.3: Details of the preheater, trajectory guide and spider leg thickness*

The thermal and mechanical properties of the die segments, which are made from steel (type SUS420J2) and the properties of the PA/GF prepreg material are given in Tables 1 and 2.

| Property | Unit | Value |
|---|---|---|
| Specific heat | J/kg.K | 460 |
| Thermal conductivity | W/m.K | 24.7 |
| Thermal expansion coefficient | 1/K | $10.3\times10^{-6}$ |
| Young's modulus | N/mm2 | 200,000 |

*Table 1: Tooling steel properties(type SUS420J2)*

| Property | Unit | Value |
|---|---|---|
| Specific heat | J/kg.K | 1183 |
| Thermal conductivity | W/m.K | 0.663 (Parallel to UD)<br>0.356 (Perpendicular to UD) |
| Thermal expansion coefficient | 1/K | $80\times10^{-6}$ |
| Viscosity (at 240°C, 10 $s^{-1}$) | Pa.s | 125 |

*Table 2: GF/PA6 basic thermal and mechanical properties*

### 3.2 FEM model development

#### *3.2.1 Meshing*

Given the geometrical dimensions of the die a 3D CAD model of the pultrusion tooling was created and then imported into LS-PrePost. For the meshing, the selected solid element mesh size for the model was made as large as possible while preserving the necessary geometric definition of the tooling. As the upper and lower dies are not symmetric about a mid-plane, they need to be meshed separately. To mesh the die set as uniformly as possible, the *Element Generation* (*Two_Shell_Sets* ) option in LS-PrePost was used. Here a quad shell mesh was first created on both ends of the die surface and then extruded in the direction of the pultrusion axis. This procedure was repeated for all the die segments having a different cross-section along their length. The completely meshed die model is shown Figure 5. The six segments of the die (upper and lower) were assigned separate part ids to assist in the better post processing of results.

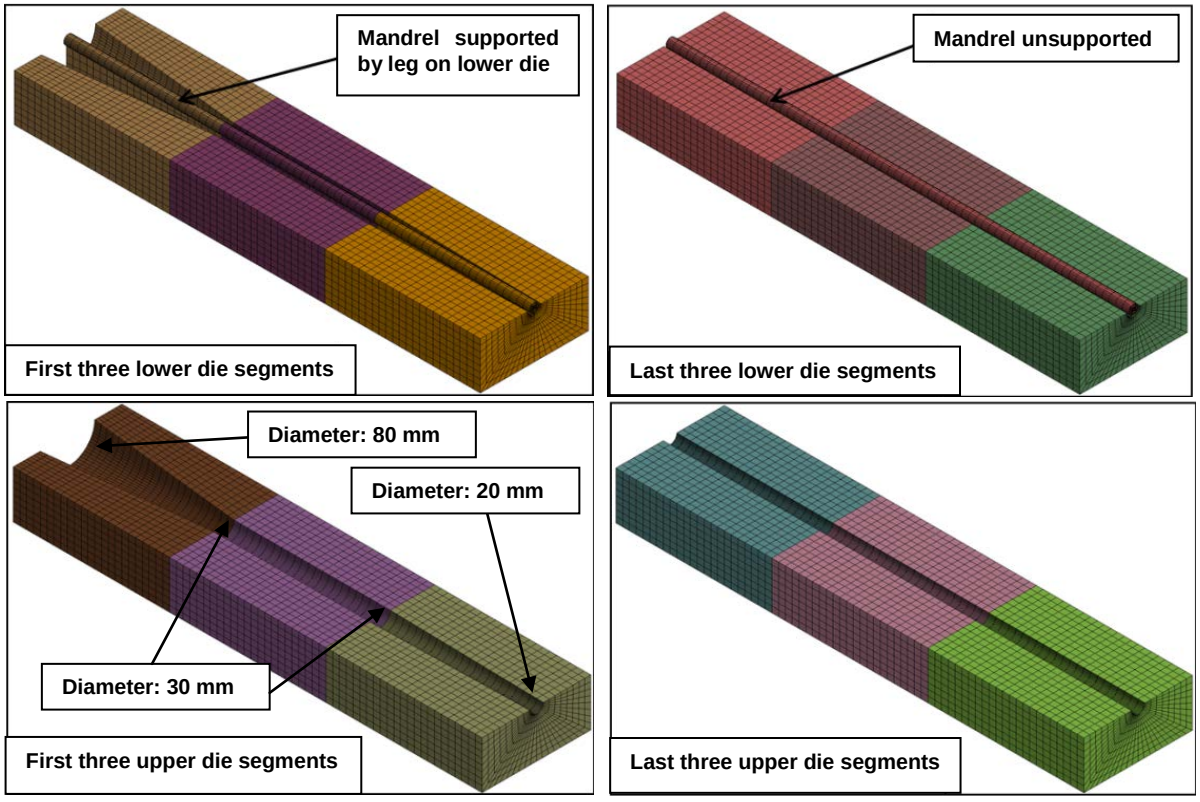


*Fig.4: Upper and lower pultrusion tool die segment meshing*

To create the mesh for the input material (unidirectional GF/PA6 prepreg), a cylindrical volume was created overlapping the Lagrangian parts (tooling dies) with at least one solid element. The meshing was again carried out using the same principle used for the die segments (*Element Generation* (*Two_Shell_Sets*)). It was also important to ensure a mesh size ratio of at least 2:1 between the ALE volume and tooling in order to avoid contact problems (best results for ALE simulations in LS-DYNA in the past have been achieved using a mesh size ratio of 4:1, at the expense of calculation time). Two variants of the ALE mesh were produced in order to investigate the influence of a higher and lower quantity of pultrusion input material. The lowest quantity of material input corresponded to the exact volume of material necessary to create the desired tubular geometry, while the higher quantity of material input corresponded to double the necessary volume. Beam elements were used to represent fibers in the form of rovings and were positioned inside the ALE fluid material. One beam element was positioned at the center of each solid element filled with the ALE fluid (PA6 polymer). Several different ALE fluid structure interaction (FSI) configurations were trialed during model development including configurations using both stationary and moving ALE volumes. The configuration which worked best involved a moving ALE mesh which translates together with the input material along the pultrusion axis. To help reduce the calculation time, an ALE volume of around half the complete length of the tooling was used for the analysis.

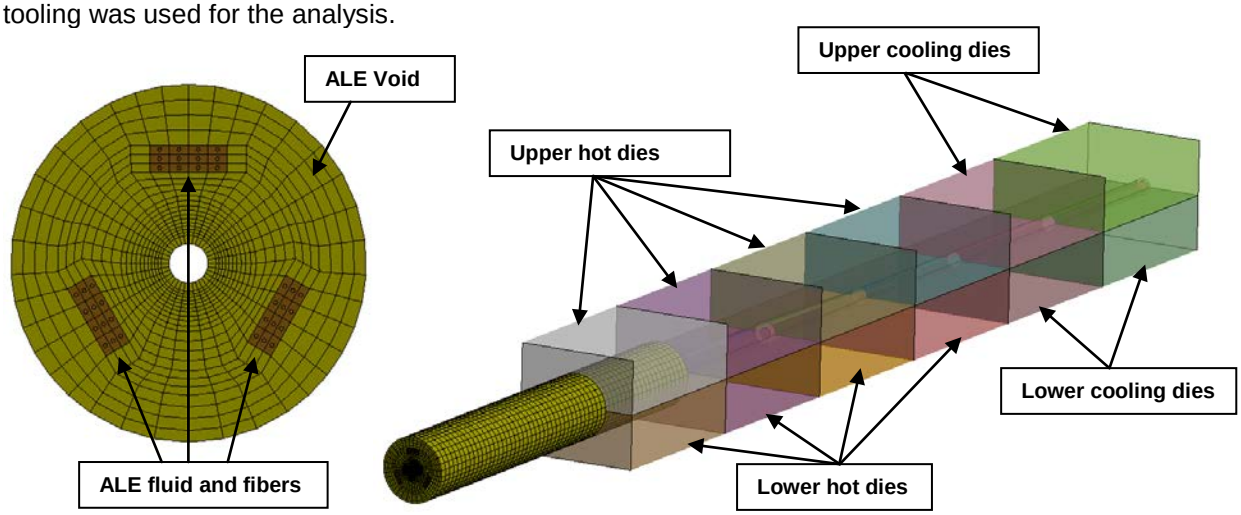


*Fig.5: Final pultrusion process simulation model mesh configuration*

### *3.2.2 ALE specific keyword definitions*

In the following section of the paper the LS-DYNA keywords used to setup the ALE pultrusion simulation model are explained in more detail. The part containing the empty cells around the ALE fluid material, into which the fluid may be transported, is called the void (as shown in Figure 5, left) and it is defined using the keyword ***INITIAL_VOID** simply by giving the part id associated with it. This part has the same material properties as the ALE fluid material and in this simulation, both the fluid and void are assigned the ***SECTION_SOLID** element formulation type 12 (1 point integration with single material and void). The ***ALE_ESSENTIAL_BOUNDARY** keyword is used to ensure no material can flow outside the defined ALE mesh volume. The ***ALE_REFERENCE_SYSTEM_GROUP** keyword specifies certain degrees of freedom for the ALE mesh. In the current model, it is set to be able to move via translation without expansion or rotations alone the pultrusion axis.

One of the most important inputs in the model is the ***CONSTRAINED_LAGRANGE_IN_SOLID** keyword card which defines the coupling mechanisms between the ALE fluid and tooling and also the ALE fluid and fibers (beam elements representing glass fiber rovings). In this simulation model, two separate ***CONSTRAINED_LAGRANGE_IN_SOLID** keyword cards are used to help setup these interactions. The first card (shown in Figure 6) represents coupling between the ALE fluid and tooling, while the second (Figure 7) shows the coupling parameters used between the ALE fluid and the fibers. In the first card, the ALE void and fluid are defined as a master set and the die tooling is defined as a slave. The coupling points (NQUAD), coupling method (CTYPE) and coupling direction (DIREC) are defined as per the LS-DYNA keyword manual guidelines. In the initial development of the simulation model, friction is not considered and is assigned a default value of zero. In later simulations, according to the amount of input material defined, friction becomes important and can be defined a value in the range of 0 to 0.2. In order to control the leakage between master and slave parts, PFAC (a contact stiffness

scaling factor), ILEAK (coupling leakage control flag) and PLEAK (leakage control penalty factor) are also adjusted. Further important parameters to be defined in this card are concerned with the heat transfer which occurs between the ALE fluid and tooling. This is defined with the help of a heat transfer coefficient (CQ) and a minimum and the maximum air gap between the ALE fluid and tooling die segments allowing heat transfer (HMAX, HMIN). All other parameters in the card are left as the defaults suggested by LSTC. In the same way, the second card for coupling the ALE fluid to the fibers is defined as shown in Figure 7. The major difference here is the CTYPE used which is set to the default type of 2 constraining the acceleration and velocity of the nodes in both these parts. The heat transfer between the fibers and fluid is not considered (but is now also possible since R11) as temperature effects on the mechanical properties of the fibers here are considered negligible.

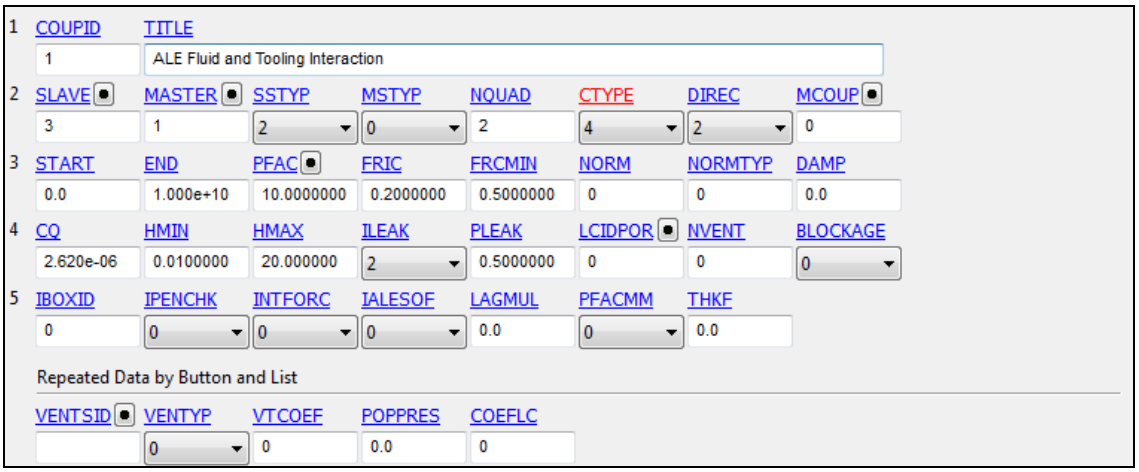


*Fig.6:* ****CONSTRAINED_LAGRANGE_IN_SOLID*** *keyword for ALE fluid to tooling interaction*

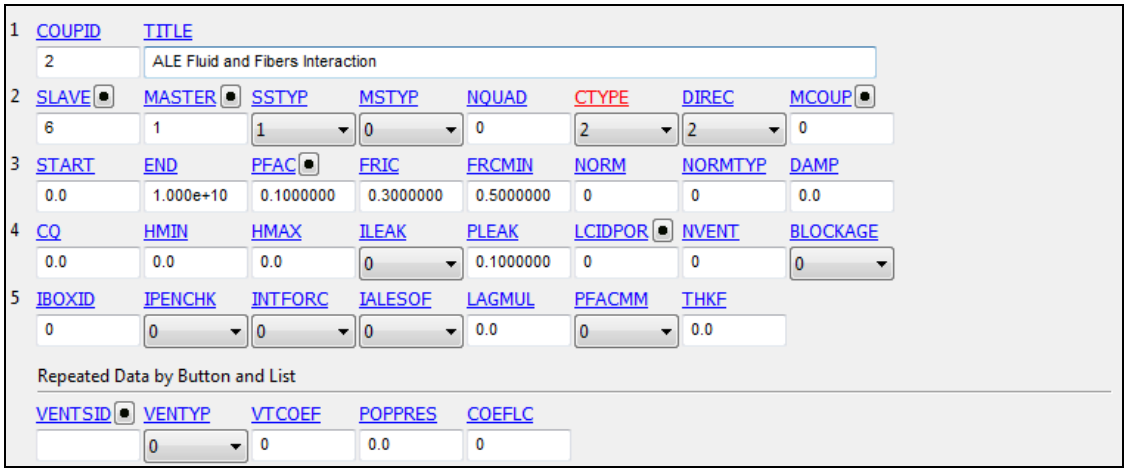


*Fig.7:* ****CONSTRAINED_LAGRANGE_IN_SOLID*** *keyword for ALE fluid to fibers interaction*

### *3.2.3 Movement boundary conditions*

To create the pulling boundary condition on the input material, the keyword ***BOUNDARY_PRESCRIBED_MOTION_SET_ID** is used. As shown in the following Figures 8 and 9, a fibers node set defined at the input end nodes of the material (NSID = 60) is given a velocity (VAD = 0) in the positive y-direction (DOF = 2). The pulling velocity versus time is then defined via a ***DEFINE_CURVE_SMOOTH** load curve (LCID = 4) as shown in Figure 9. It can be seen that the base pulling speed of 0.2 m/min (0.0033 m/s) is in this case simulated at 3 m/s (3 m/s) several hundred times faster than reality in order to make the calculation time feasible. This is still below the speed at which inertial effects come into play. The correct thermal behavior is ensured through the use of a thermal speed up factor (TSF) found in the ***CONTROL_THERMAL_SOLVER** keyword card. Note that the unit system used throughout the development of the model here is **mm-kg-ms-KN-GPa**.

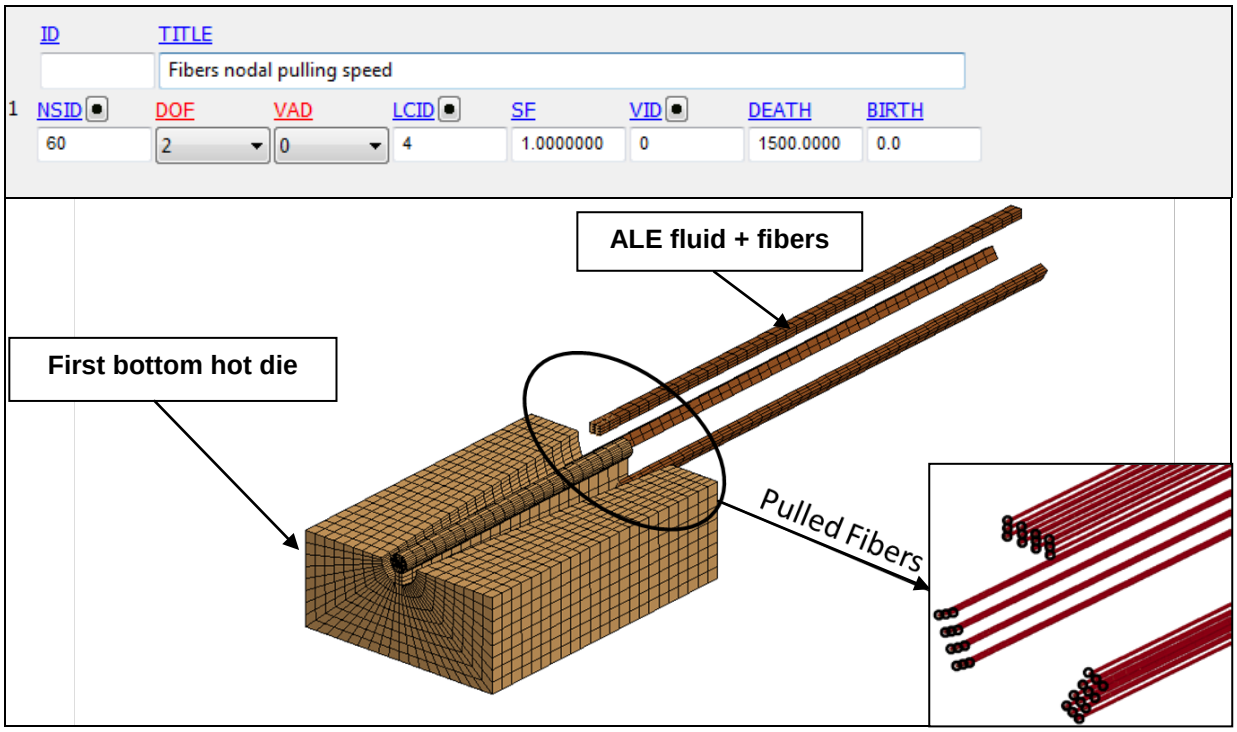


*Fig.8:* ****BOUNDARY_PRESCRIBED_MOTION_SET_ID*** *keyword defining pulling speed BC*

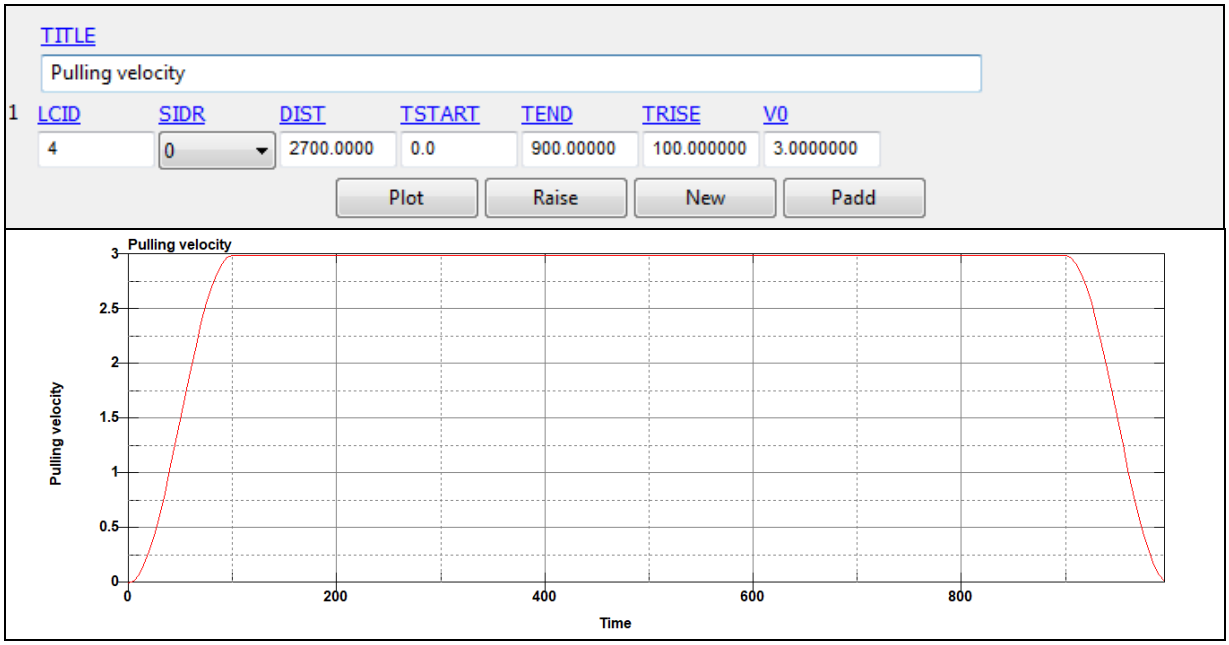


*Fig.9:* ****DEFINE_CURVE_SMOOTH*** *keyword used to define the pulling speed velocity profile*

### *3.2.4 Thermal boundary conditions*

As per the provided input data, the hot die segments were set to 240°C (513K) and the cooling die segments at room temperature (here considered to be 27°C (300K)). For the thermal/structural analysis, these temperature boundary conditions are defined via the keyword ***BOUNDARY_TEMPERATURE_SET**. As shown in Figure 10, nodes of the hot die segments represented by node set 2, reference a curve via the ***DEFINE_CURVE** keyword defining a constant temperature of 513K on the part and likewise for node set 3 300K on the part. In addition, for each part, the initial temperature was also defined via the ***INITIAL_TEMPERATURE_SET** keyword card as shown in Figure 10. The void, fibers and fluid were all give an initial temperature of 150°C (423K), which is the temperature of the input material as it leaves the preheating unit.

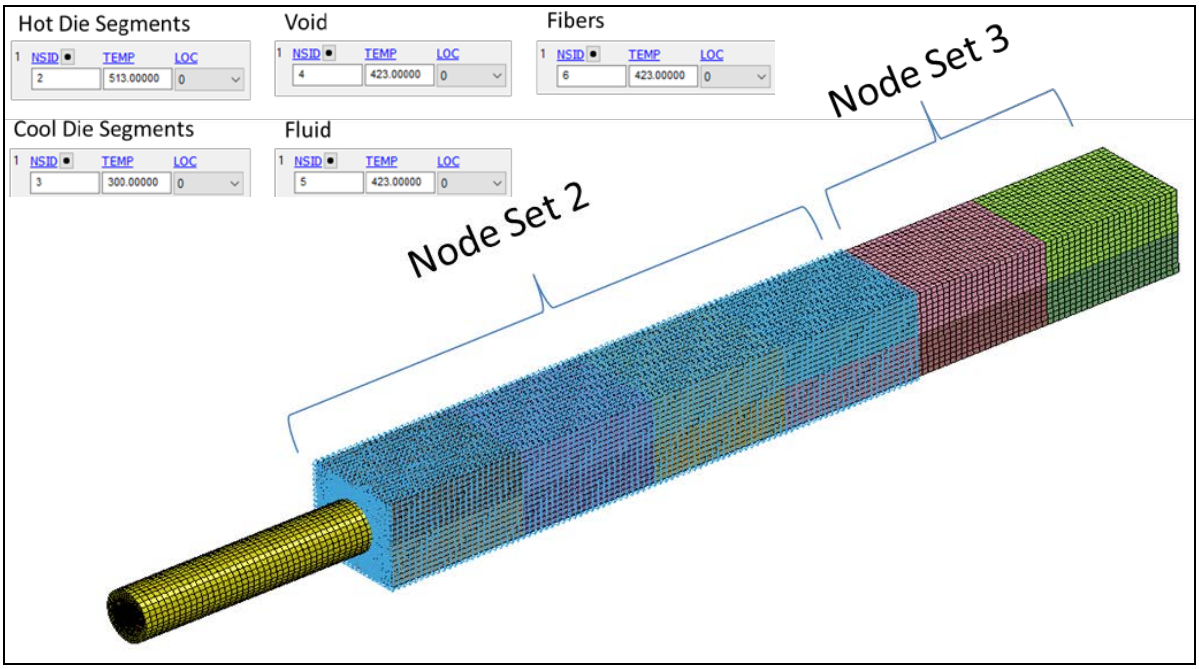


*Fig.10: Thermal boundary conditions applied to the pultrusion model*

### *3.2.5 Section definitions*

The model contains two types of elements, solid and beam elements. The fibers embedded in the input material are described using 1D beam elements (via ***ELEMENT_BEAM**) and the ***SECTION_BEAM** keyword card defines how the cross-sectional properties are defined. The default element formulation (ELFORM) 1, cross section type (CST = 1) type tubular with an outer diameter of 1 mm was assigned. Likewise, the section properties for the solid ALE fluid elements, void and die segments are defined via the ***SECTION_SOLID** card. For the ALE simulation, the void and ALE fluid elements have the same section properties (ELFORM = 12) assigned (1 point integration with single material and void). As the die segments are rigid, they are assigned the default constant stress solid element (ELFORM = 1).

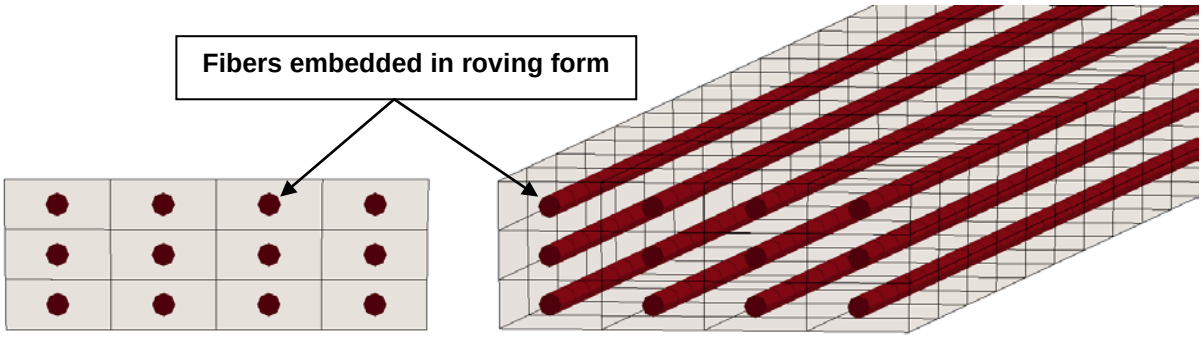


*Fig.11: Definition of fibers as clustered rovings using solid tubular beam elements*

### *3.2.6 Material model definitions*

Perhaps the most important part of the simulation is the material model definition for each part. In the first stage of simulation model preparation, the aim was to define simple material models for each part. Once again, the unit system used throughout the keyword definition is **mm-kg-ms-KN-GPa**. This means that, length is defined in 'mm', mass in 'kg', time in 'ms', force in KN and an elastic modulus in GPa. The die segment elements are assigned the ***MAT_RIGID (*MAT_020)** material model card, as the die parts are made of steel and are at present not considered to deform. As shown in Figure 12, the material model card, density (RO), elastic modulus (E), Poisson's ratio (PR) have been defined for steel (SUS420J2). Furthermore, to constrain all degrees of freedoms of the part, the constraint parameters (CON1 und CON2) are assigned the values for this condition respectively, (see Figure 12).

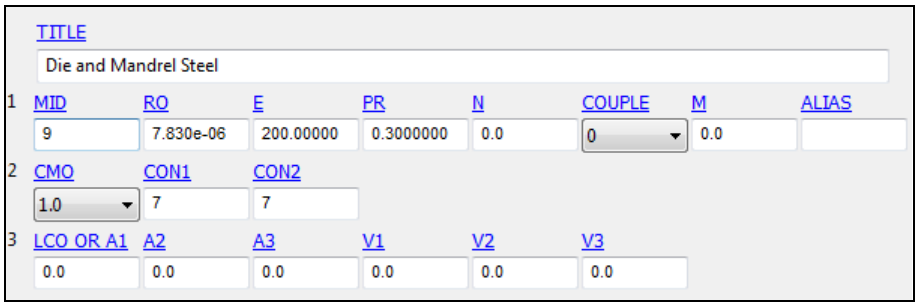


*Fig.12: Tooling material model (***MAT_RIGID**)*

The fibers are defined with the ***MAT_ELASTIC** (or MAT_001) keyword card. As shown in Figure 13, the material properties density (RO), elastic modulus (E), Poisson's ratio (PR) is defined for glass fibers. The density and stiffness values are however reduced by a factor of 10 to ensure the bending stiffness of the roving is not overestimated due to its solid cross-section and to help improve the overall simulation time step (i.e. to reduce the simulation time).

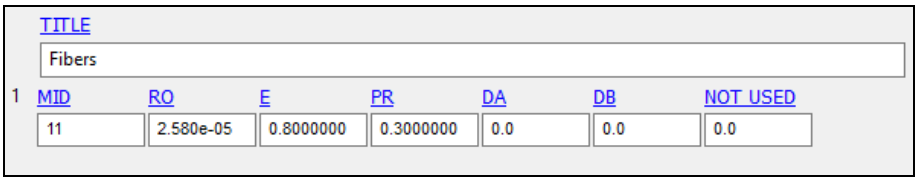


*Fig.13: Fiber (Roving) material model (***MAT_ELASTIC**)*

The material model definition for the ALE fluid material or thermoplastic polymer is a complex task. As described in the input data Section 3.1, the material temperature varies from 150°C to 240°C and then from 240 °C to 25°C. During this process, the thermoplastic polymer melts and shear thinning effects take place. The material behavior at higher temperature is partially viscoelastic and viscoplastic. Due to the unavailability of detailed experimental data at temperatures above 150°C, it is difficult to define the material model completely over such a wide temperature range. Three different material models (***MAT_ELASTIC_PLASTIC_THERMAL,** ***MAT_INV_HYPERBOLIC_SIN** and ***MAT_ELASTIC_VISCOPLASTIC_THERMAL**) were tested, however, in order to setup a basis simulation model, the simplest material model ***MAT_ELASTIC_PLASTIC_THERMAL** was used. As shown in Figure 14, the ALE material property at each temperature (T1 to T8), including the Elasticity modulus (E), Poisson's Ratio (PR), initial yield stress (SIGY) and tangent modulus (ETAN) are all specified. The defined values are approximate values defined as per data sheets available for similar materials found in the CAMPUS® plastics material database.

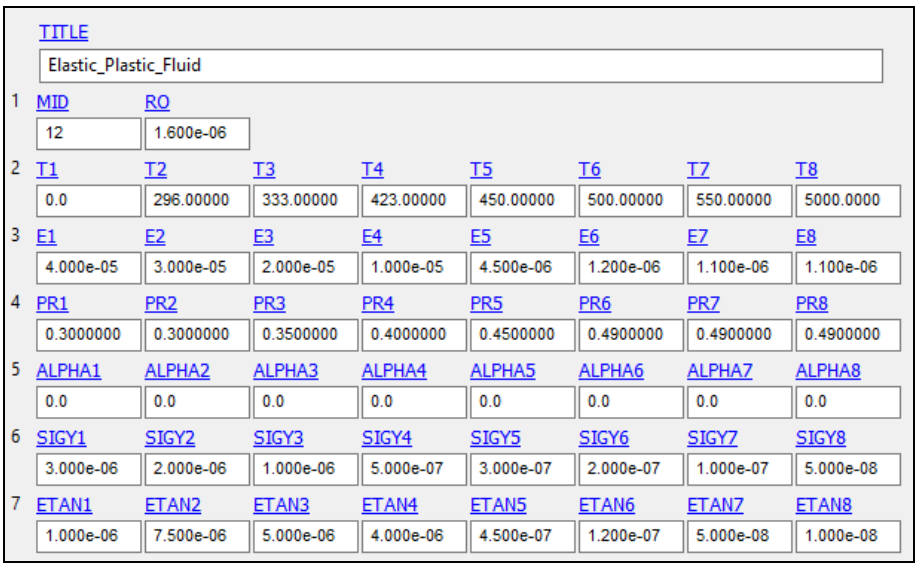


*Fig.14: Input variables for the thermoplastic polymer (PA6) (***MAT_ELASTIC_PLASTIC_THERMAL**)*

A more complex material model ***MAT_ELASTIC_VISCOPLASTIC_THERMAL** can also be used to define the behavior of ALE fluid during the process. This material model is defined with an effective stress vs. plastic strain curve (LCSS), the temperature dependence of Elasticity modulus (E), Poisson's ratio (PR) and initial yield stress (SIGY) can also all be defined with load curves LCE, LCPR and LCSIGY. ***MAT_INV_HYPERBOLIC_SIN** provides a further more complex function based option for defining the necessary material properties. Apart from the mechanical properties, thermal properties such as the specific heat (HC) and thermal conductivity (TC) of the thermoplastic polymer material (ALE), steel die segment blocks and glass fibers also need to be specified. This done via the ***MAT_THERMAL_ISOTROPIC** keyword card. The defined properties for each part are shown in the Figure 15.

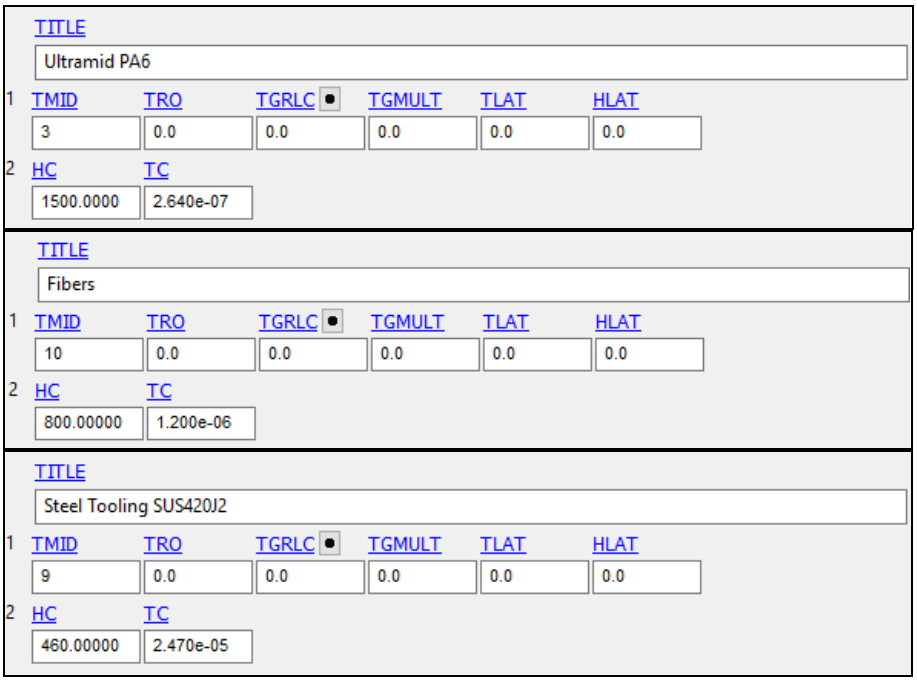


*Fig.15: Polymer, fiber and Tooling thermal property definitions using ***MAT_THERMAL_ISOTROPIC***

### *3.2.7 Control card definitions*

With the ***CONTROL_SOLUTION** keyword card, the type of analysis solution procedure is defined. For a structural only analysis, SOLN 0 is selected, while for a coupled structural thermal analysis SOLN 2 is selected. All other factors are kept default as shown in Figure 16.

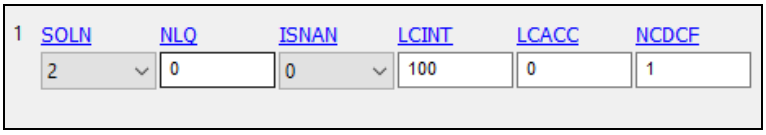


*Fig.16: ***CONTROL_SOLUTION** keyword definition*

To define the timeframe for the simulation model ***CONTROL_TERMINATION** is used, as shown in Figure 17. The 'ENDTIM' parameter is set to 600ms.

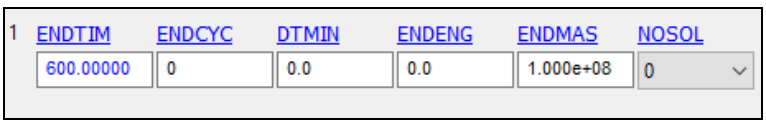


*Fig.17: ***CONTROL_TERMINATION** keyword definition*

With the help of different options in the ***CONTROL_THERMAL_SOLVER** card, the more in-depth thermal analysis parameters such as the type of analysis, convergence tolerance, thermal speedup factor etc. are all defined. As shown in Figure 18, a transient analysis linear thermal problem is defined and the thermal solver parameters are given as ATYPE = 1, PTYPE = 0 and SOLVER =1 respectively.

A thermal speedup factor is applied so that the thermal properties are adjusted for the higher pulling speed used in the simulation. The defined pulling speed is nearly 1000 times higher than the actual process speed (to allow the calculation to take place within a reasonable timeframe), the thermal properties are therefore adjusted accordingly by setting TSF = 1000.

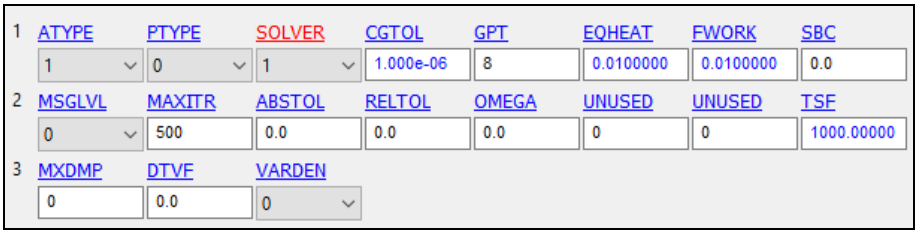


*Fig.18:* ****CONTROL_THERMAL_SOLVER*** *keyword definition*

In the ***CONTROL_THERMAL_TIMESTEP** keyword card a fixed thermal time step (TS = 0) is set together with an initial thermal time step (ITS = 2) of 2 (see Figure 19). As the thermal calculation in LS-DYNA is implicit, there is no upper limit on thermal time step size.

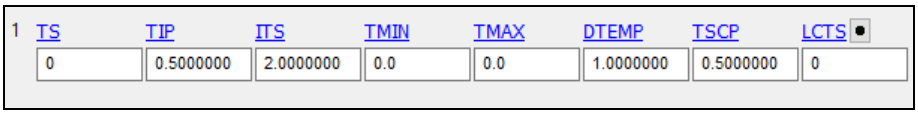


*Fig.19:* ****CONTROL_THERMAL_TIMESTEP*** *keyword definition*

The structural time step is defined with the ***CONTROL_TIMESTEP** keyword card. As shown in Figure 20, DTINIT = 0 indicates that LS-DYNA automatically calculates the initial step size and the TSSFAC is a time step scaling factor set to 0.5 (below the default value of 0.9) to improve the stability due to the large number of contacts and interactions present in the model.

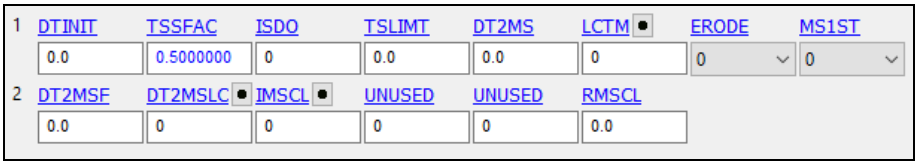


*Fig.20:* ****CONTROL_TIMESTEP*** *keyword definition*

### *3.2.8 Database card definitions*

In order to write the output data in different forms for the pultrusion model, database keywords also need to be defined. With the ***DATABASE_OPTION** card, various ASCII files can be written. By defining BNDOUT, GLSTAT, MATSUM, RCFORC, TPRINT etc., boundary condition forces and energy, global data, material energies, resultant internal forces and thermal outputs can all be obtained respectively. For example, TPRINT (Beam energy balance information) is defined as shown in Figure 21, where DT is the time interval between the desired outputs and BINARY and IOOPT are defined as per the manual guidelines. In the same way, other database outputs as mentioned above can also be created.

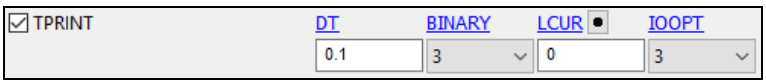


*Fig.21:* ****DATABASE_OPTION*** *keyword definition*

Using ***DATABASE_BINARY_D3PLOT,** histories of the geometry and other state variables can be used to animate and plot histories of element stresses and nodal displacements. NPLTC defines the number of .d3plot files to be created; whereas the number of animation plots can be defined via the DT or NPLTC parameter (note that NPLTC overwrites DT). Figure 22 shows in this case 60 plots have been defined for the model.

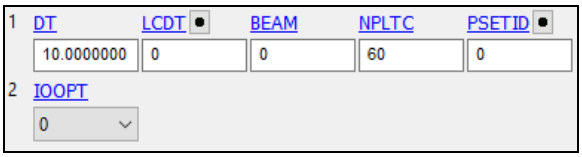


*Fig.22:* ****DATABASE_BINARY_D3PLOT*** *keyword definition*

In order to control the content of the BINARY D3PLOT output database, the ***DATABASE_EXTENT_BINARY** card is used. As shown in Figure 23, there are many factors which can be controlled. STRFLG is used to control the writing of plastic strain data to the .d3plot file. Furthermore, the parameter THERM is used to control the thermal data which is written.

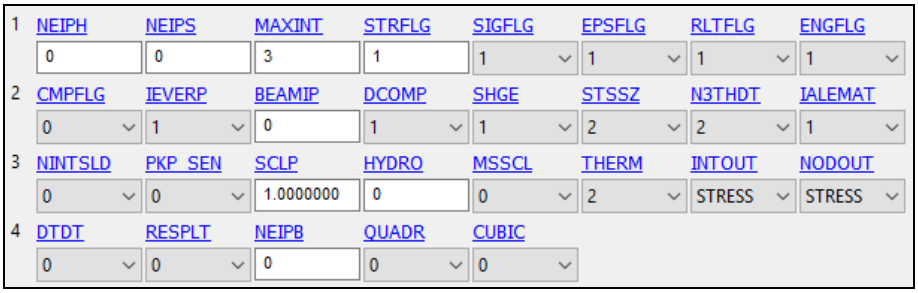


*Fig.23:* ****DATABASE_EXTENT_BINARY*** *keyword definition*

With the ***DATABASE_FSI** keyword card, the interaction between the Lagrangian and ALE parts can be obtained. The sampling time for the average pressure calculation between the various dies and the input material is calculated as per the parameters given in this card. For example, as shown in Figure 24, for each time interval DT = 0.1, the interaction parameters such as average pressure, coupling force are obtained between part ID 1001(the 1st lower die segment) and the ALE part. Similarly, this card is therefore defined for all the tooling die segments.

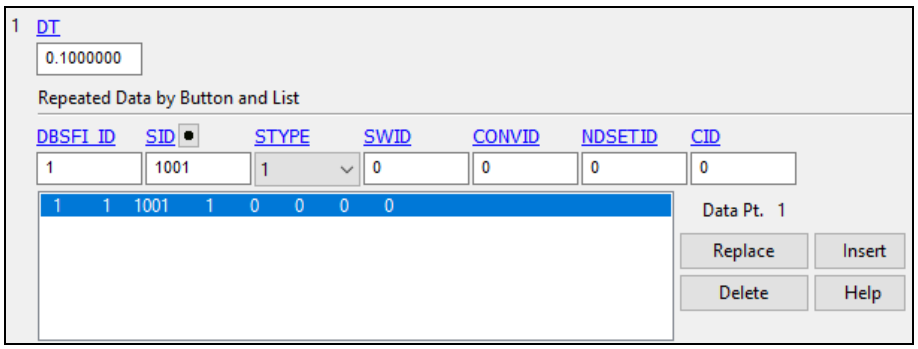


*Fig.24:* ****DATABASE_FSI*** *keyword definition*

### 3.3 Final simulation model

After the complete definition of the keyword cards, the final simulation models required for obtaining pressure and temperature profiles at different processing speeds were created. Two base simulation models were prepared, one containing a *minimum* and the other a *maximum* amount of input material as shown in Figures 25 and 26. The minimum cross-sectional area of prepreg input material required to form the desired tube geometry (20 mm in diameter and 3 mm thick) is 160 $mm^2$. To account for compaction, two ALE fluid mesh geometries were created, one with a 175 $mm^2$ cross-section (*minimum)* and the other with a 350 $mm^2$ cross-section (*maximum)* defining the amount of input material. These two base models were then used to check the contact stability of the developed model at the base pultrusion speed.

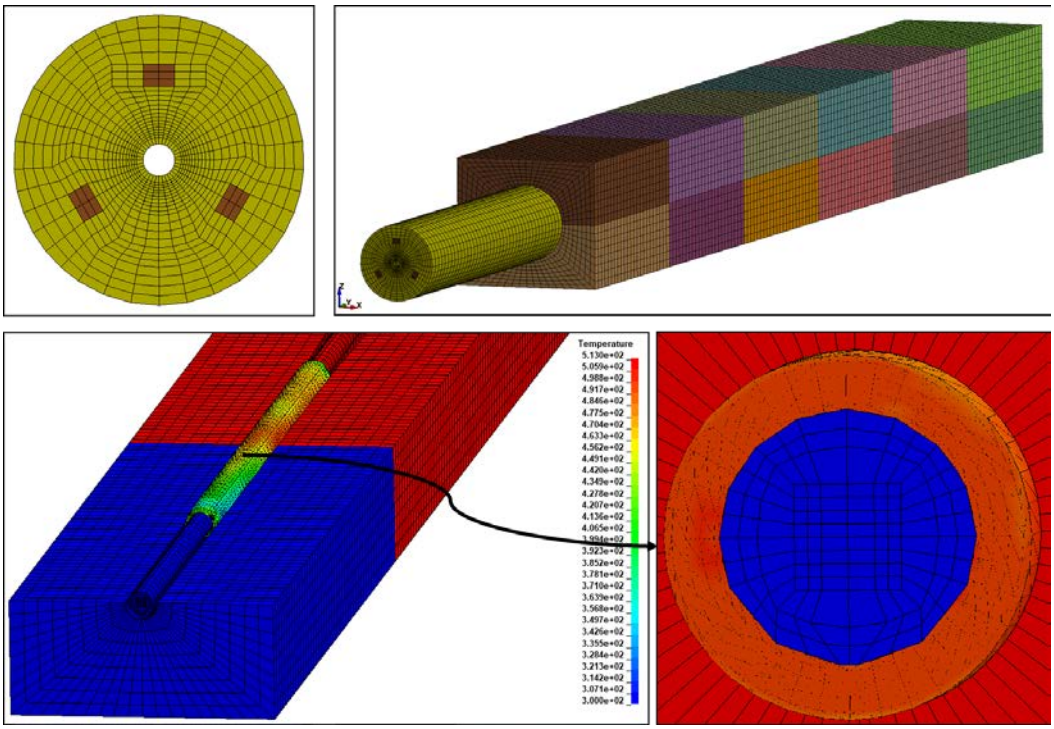


*Fig.25: Result of tube formation in simulation model with minimum material input (175 mm$^2$)*

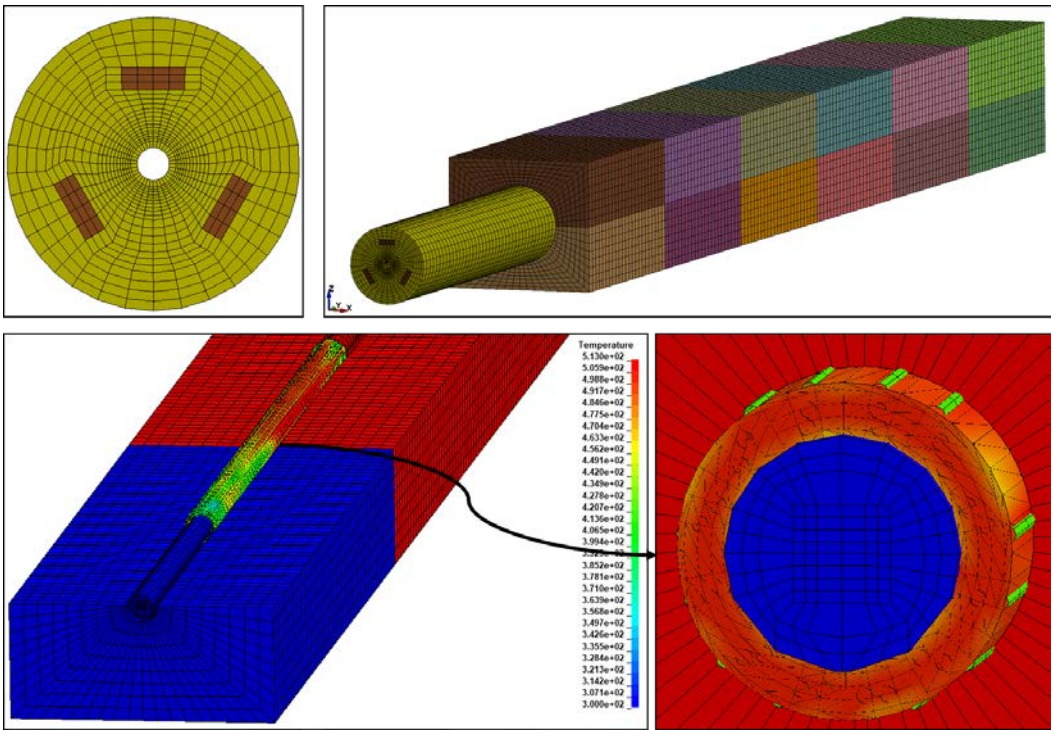


*Fig.26: Result of tube formation in simulation model with maximum material input (350 mm$^2$)*

In both cases, a finite length of input material is simulated 430 mm long, with 30 mm of material already inside the 1st die segments (where first contact occurs) and 400 mm of input material outside the tooling at the start of the simulation. The ALE void volume is made larger (600mm) than the fluid length to ensure the ALE fluid remains within the volume as it reduces in size in the radial direction and lengthens during the pultrusion to the required size of the tube, see Figure 27. This amount of material is enough to represent the process and can of course be made larger at the expense of

simulation time which was around 4.5 hours (using all 6 Cores/12 threads on an Intel® Core™ i7-6800K CPU @3.40GHz, 64GB ram).

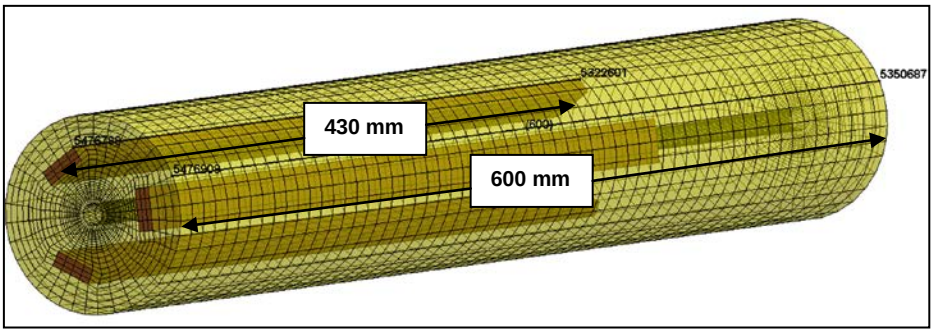


*Fig.27: Quantity of input material simulated*

Another factor considered during initial runs of the simulation was the inclusion of friction between the tooling and ALE fluid. The friction coefficient is defined in the ***CONSTRAINED_LAGRANGE_IN_SOLID** keyword card. For the minimum material input, the friction coefficient between the tooling and ALE fluid was set to 0.05 and between the ALE fluid and fibers 0.1, while for the maximum material input these parameters were set to 0.2 and 0.3 respectively. A comparison of the results of the friction study regarding the contact stability and correct formation of the hollow tube for the minimum material input are shown in Figure 28.

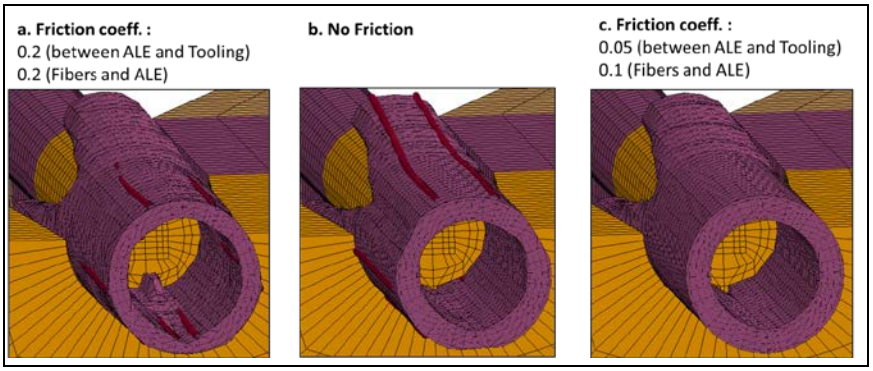


*Fig.28: Calibration of friction coefficients between ALE fluid and tooling and fibers and fluid*

To further improve the contact stability of the model and to avoid the penetration of beam elements into the tooling (as can be seen in Figure 28 a and b) a further contact definition card ***CONTACT_CONSTRAINT_NODES_TO_SURFACE** was defined to establish a contact interaction between the fibers and tooling. Here no friction values were assigned and the card consists almost completely of default values as shown in Figure 29.

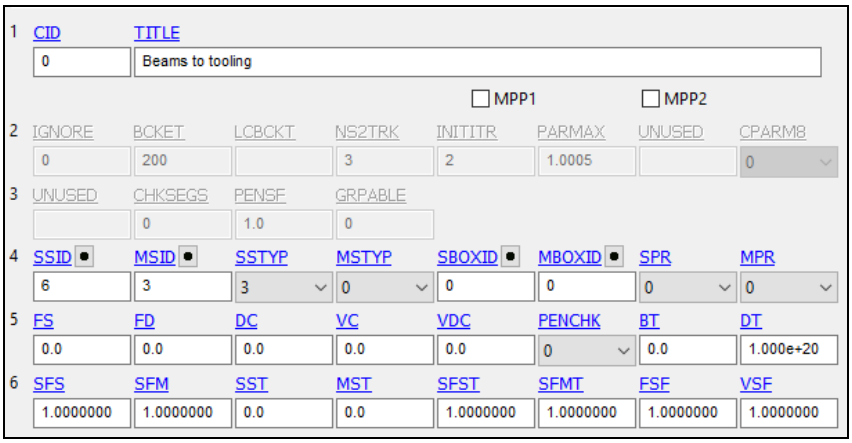


*Fig.29: ***CONTACT_CONSTRAINT_NODES_TO_SURFACE** defined for fiber to tooling contact*

## 4 Parameter study results

As shown in the previous section, two models have been developed for studying the effect of a minimum and maximum amount of pultrusion material input. In order to obtain the temperature and pressure profiles at various speeds, multiple simulations with these models were carried out. The results obtained from the study are presented in this section.

### 4.1 Temperature profiles for minimum material input model

The variation in the input material temperature over the entire length of the pultrusion die at various speeds can be examined as shown in Figure 30. The main focus is the maximum temperature reached by the ALE fluid part at the end of the hot die segments; therefore the simulation state at that location is considered in detail for analysis.

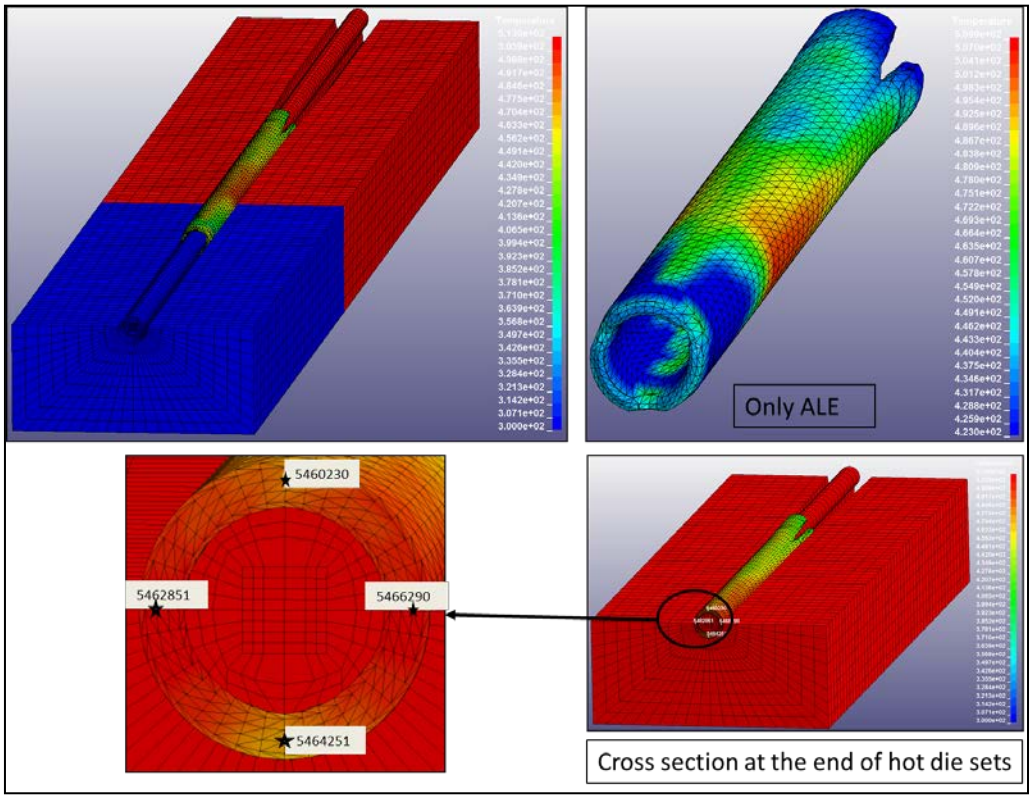


*Fig.30: Temperature distribution at base pulling speed (Max. temp. 509K) for minimum material input*

Temperature plots of single nodes at various radial positions in the middle of the tube thickness versus die length are selected for the creation of the temperature profile plots, one of which (Node 5462851) is shown in Figure 31. The trends exhibited in the curves shows good agreement with studies found in the literature [3] [10] [11]. As the tooling has also been simulated, it is possible to compare temperature curves in different regions within the volume of the profile. This can become important for more complex geometries to decide where to best position heating elements within the tooling. Another important observation is the effect of pulling speed on the temperature profile. It can be seen from the plot, (Figure 31), that an increase in pulling speed leads to a drop in maximum temperature. This is because the material residence time within the hot die segment decreases as the speed increases and therefore there is less time for heat transfer to take place between the tooling and the material. The trend in the maximum temperature development of the material in relation to the pulling speed is in agreement with the experimental study carried out by Tanaka et al. [10]. In the present simulation model, the maximum temperature reduces from 509K at the base pulling speed to 488K, 461K and 446K for 2x, 4x and 6x the base pulling speed respectively.

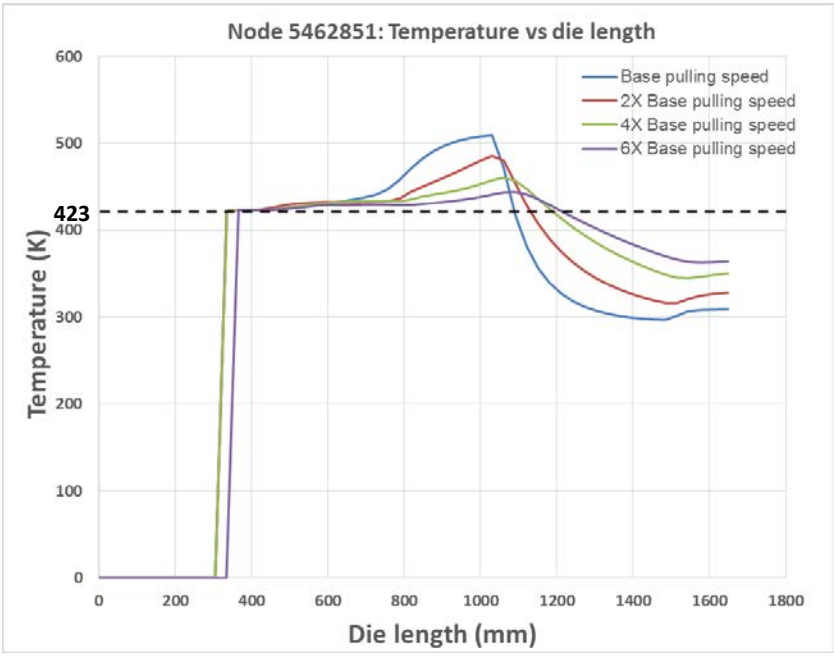


*Fig.31: Node 5462851: Temperature vs. die length for minimum material input*

### 4.2 Temperature profiles for maximum material input model

With double the material input, the effects of pulling speed are similar to that explained in the previous Section 4.1. A further observation that can be made by comparing each model at the same speed is the effect of the material increase on the temperature profiles. When comparing the temperature distribution within the part in the two models for the base pulling speed, (Figures 30 and 32), it can be clearly seen that in the maximum material input model, the temperature is higher and more uniform.

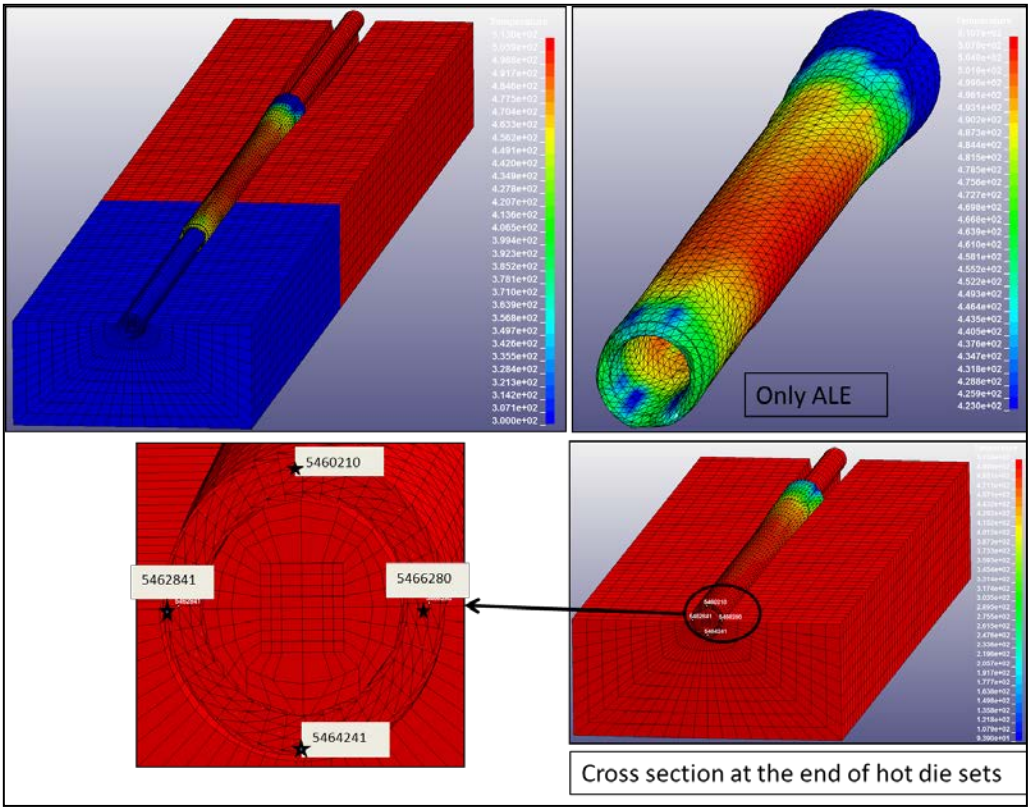


*Fig.32: Temperature distribution at base pulling speed (Max. temp. 509K) for maximum material input*

Furthermore, the maximum temperature reached at 2x and 4x the base speed for the minimum material input model (488K and 461K) are both lower compared to the maximum material input model (497K and 472K) as shown in Figure 33. It was not possible to run the maximum material input model at 6x the base speed due to numerical instabilities resulting from very high increases in material pressure which can be seen later in Section 4.4. It is almost certain that this configuration (maximum material input and 6x the base pulling speed) is also not possible in reality given the fixed temperature boundary conditions in the tooling.

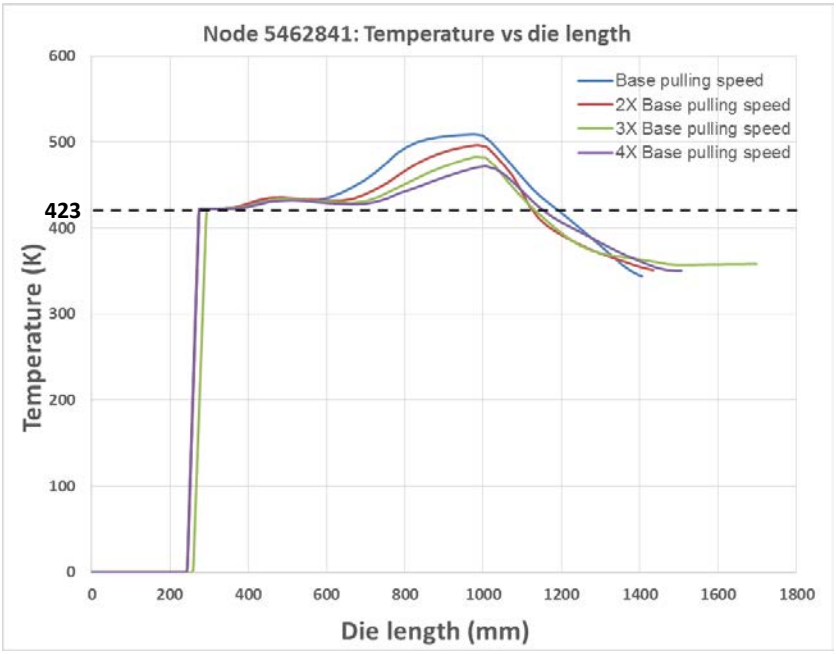


*Fig.33: Node 5462851: Temperature vs. die length for maximum material input*

### 4.3 Pressure distribution profiles for minimum material input model

The pressure on the input material is an important parameter which can be analyzed for the two material input models which have been created and also at the various pulling speeds. Only the first four hot die segments are considered here in order to analyze pressure trends rather than quantitate values. Here the material has been assigned the most realistic material property (stiffness values) based on the temperature it experiences in these four dies. At the cooling dies, although thermally correct, the input material remains soft (i.e. in the simulation the phase change from molten to solid is not modeled in terms of stiffness due to the unavailability of material data). Therefore the pressure trends in this area are not considered. In any case, the material in the cooling dies is not expected to experience high pressure due to the fact that the profile remains constant in this region of the die and due to material thermal contraction (currently also not considered in the model). Given this argument, the time step in the pultrusion simulation model can be kept reasonable by keeping the stiffness input low. In addition, experimental pressure data measurements are also not at present available. In order to obtain a quantitative output from the simulation, a thorough input material characterization and process validation using temperature and pressure sensors mounted on the actual pultrusion equipment needs to be carried out.

The pressure distribution on the ALE fluid at simulation state at the end of hot die segments at different processing speeds for the minimum material input is shown in Figure 34. It can be seen that the pressure distribution becomes more uneven at higher pulling speeds which could lead to problems in the part (e.g. void defects or surface quality). Furthermore, for each die segment block (top and bottom) the average contact pressure profiles can be plotted and compared for various pulling speeds as shown in Figures 35 and 36. Here it can be seen that in hot die 4 (both upper and lower dies) the highest material-to-tooling contact pressures occur. As the ALE fluid starts 400 mm outside the first tooling die and the simulation runs until the material travels a further 300 mm outside the last cooling die segment, the total travel length of the input material is approximately 1650 mm. This is longer than total die length (1380 mm). The plots in Figures 35 and 36 therefore show the average pressure on ALE fluid length of 430mm in each die block region against the total travel length of the ALE fluid

(1650 mm). To interpret the results in a more understandable form one can also plot the maximum pressure value (being careful to avoid any unrealistic spikes caused by numerical contact instabilities) in each die block against the material travel length at different speeds as shown in Figure 37.

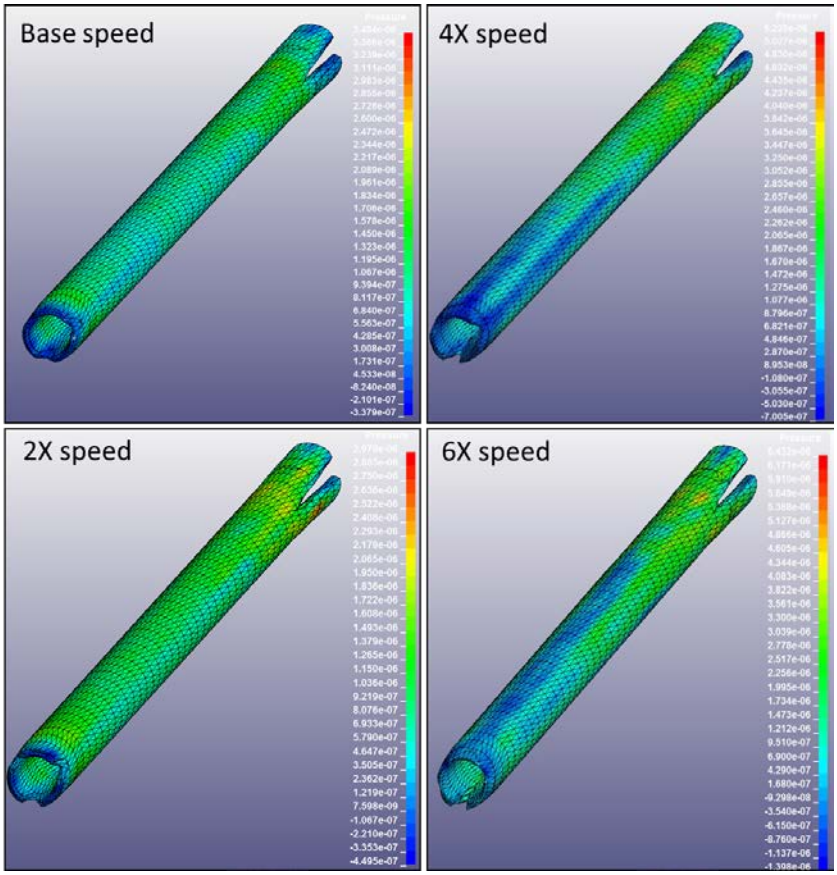


*Fig.34: Pressure contour plots at equivalent simulation state at different pulling*

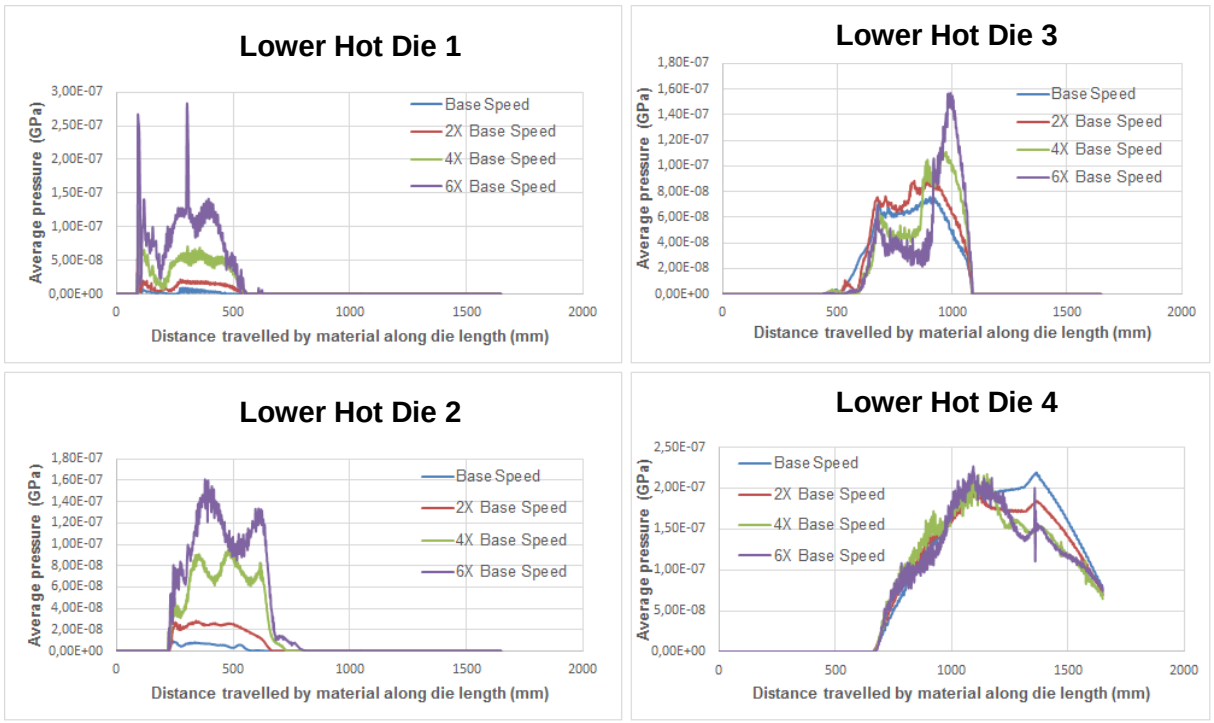


*Fig.35: 2D pressure plots for each lower hot die at different pulling speeds*

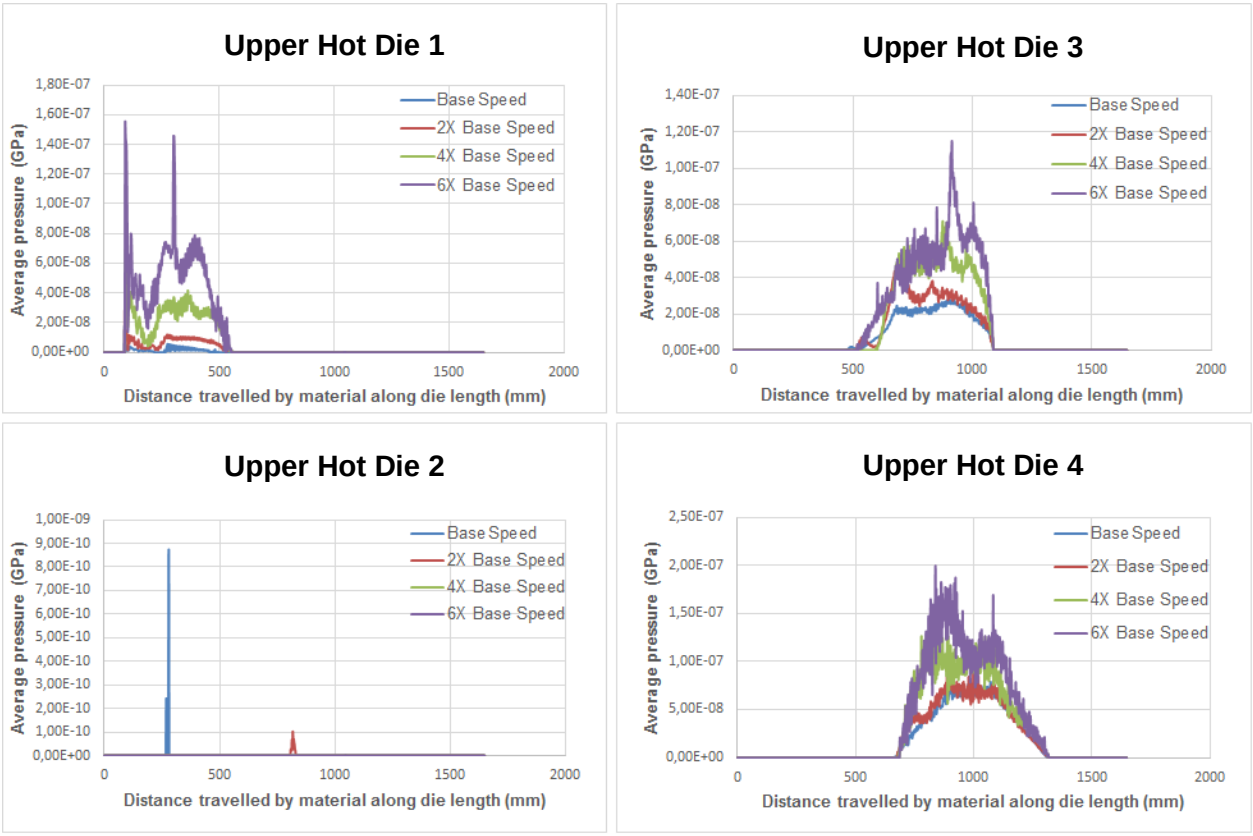


*Fig.36: 2D pressure plots for each upper hot die at different pulling speeds*

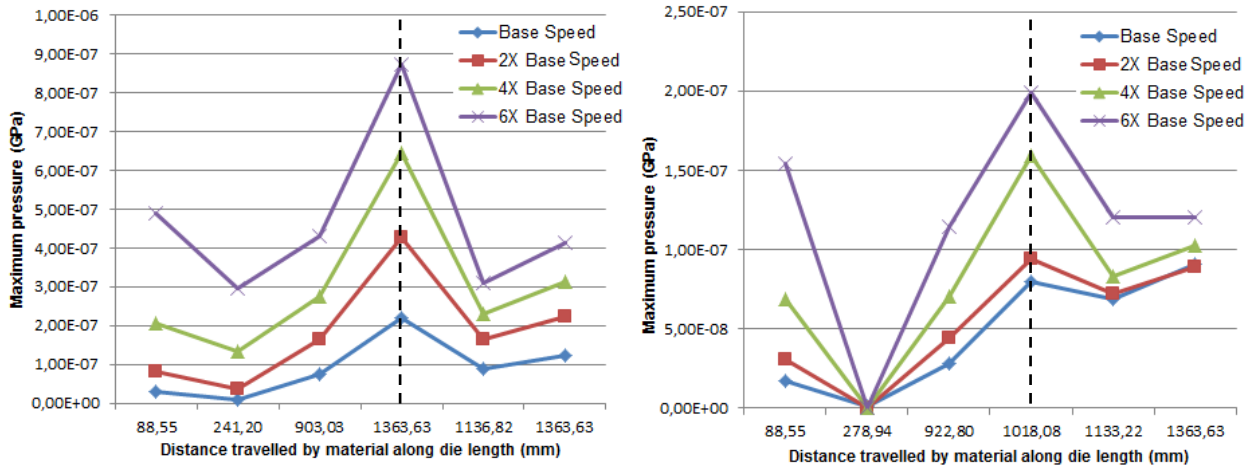


*Fig.37: Maximum pressure in the 6 lower (left) and 6 upper (right) dies vs. distance travelled by material along the die length*

From Figure 37 it can be seen that the maximum pressure experienced by the lower die is more than four times higher in magnitude than that of the upper die. In addition, the position of the maximum contact pressure for the upper and lower dies does not occur at the same position. The results confirm the highest pressure zones to be in the latter part of the 3rd hot die and 4th hot die. Note that each plotted point represents the maximum value for one of the dies. It can also be seen that the maximum pressure for the first cold die (the fifth point 1136,82 mm which appears to be incorrectly out of place) occurs when the material first arrives at that point rather than in the hot dies which show a maximum is reached when a certain quantity of material has already passed this area.

### 4.4 Pressure distribution profiles for maximum material input model

The effects of pulling speed on the pressure profiles for the maximum material input model follow a similar trend to those of the minimum material input model. The pressure distribution and pressure plots for this case are shown in Figures 38-41 and can be seen to be much higher than that of the minimum material input model. In this model, the maximum simulated pulling speed was only 4x that of the base speed. A model at 6x the base pulling speed was not possible to run without numerical contact problems.

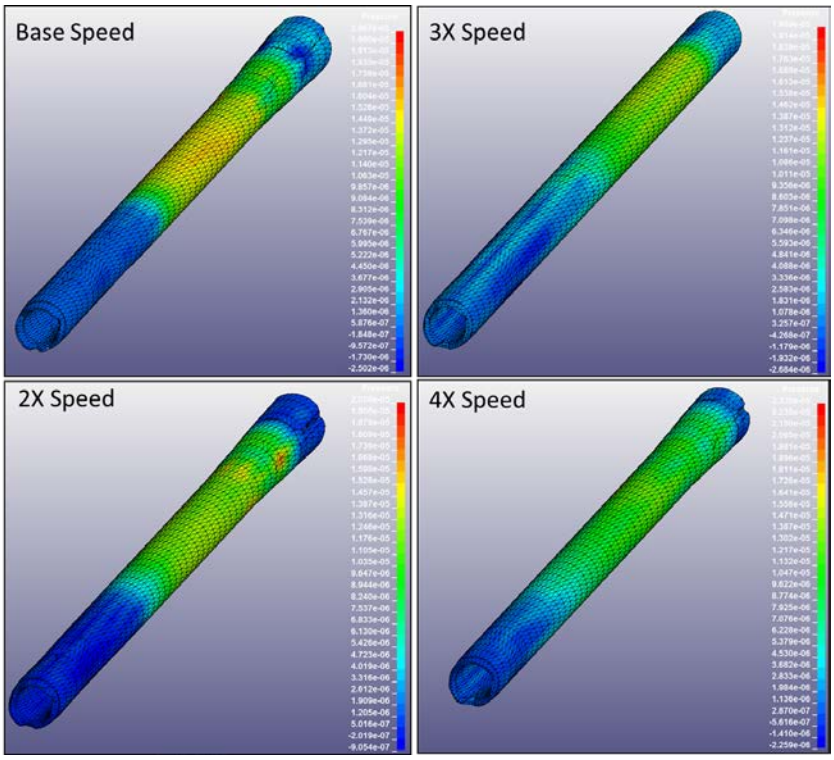


*Fig.38: Pressure contour plots at equivalent simulation state at different pulling speeds*

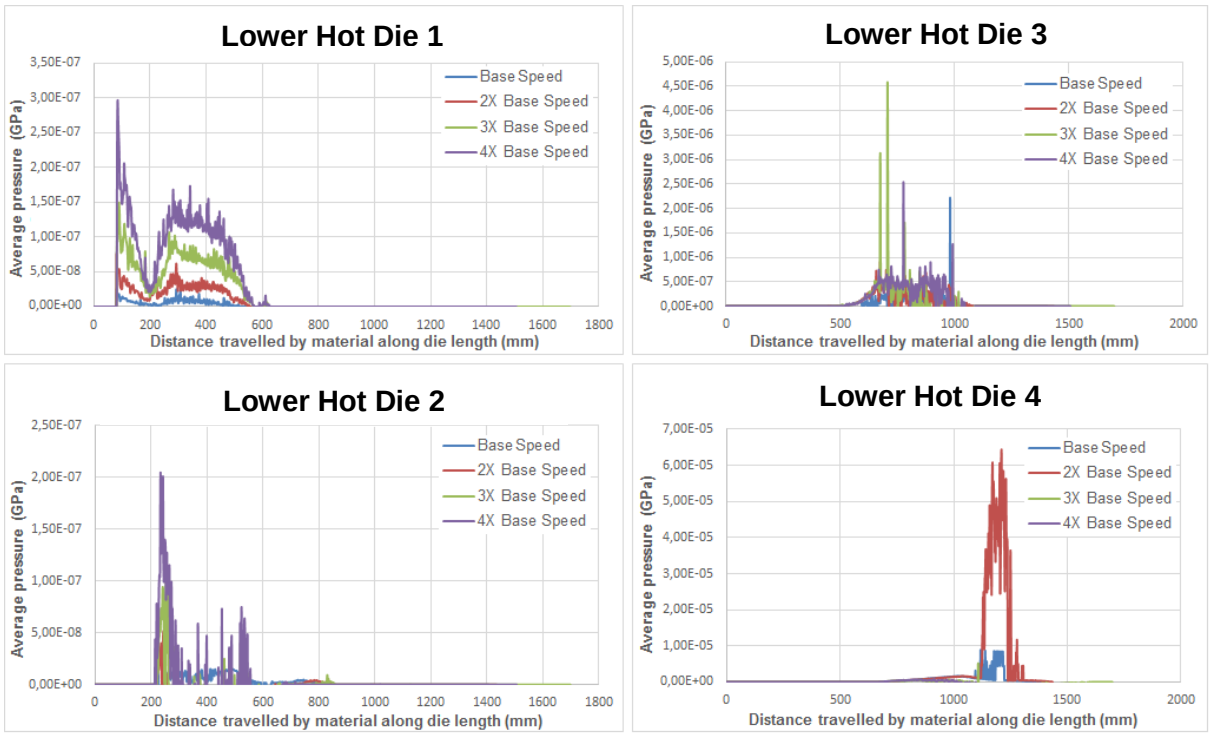


*Fig.39: 2D pressure plots for each lower hot die at different pulling speeds*

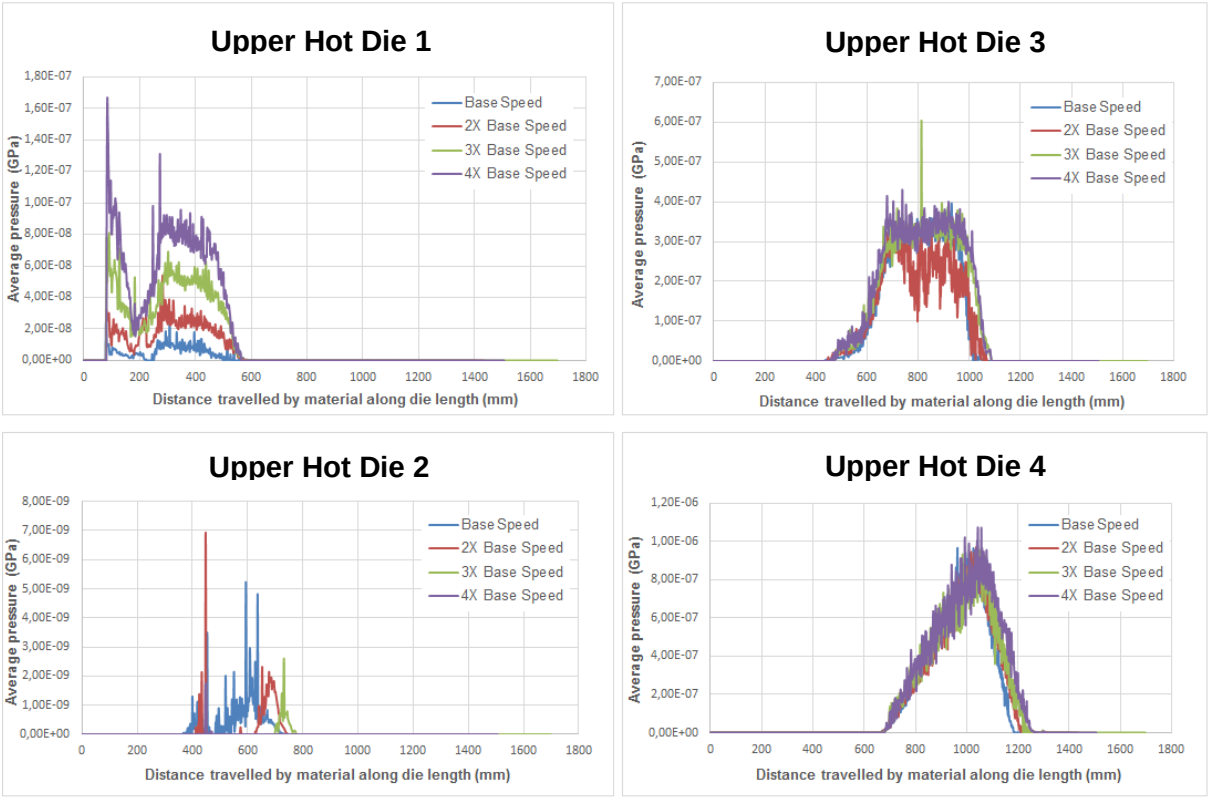


*Fig.40: 2D pressure plots for each upper hot die at different pulling speeds*

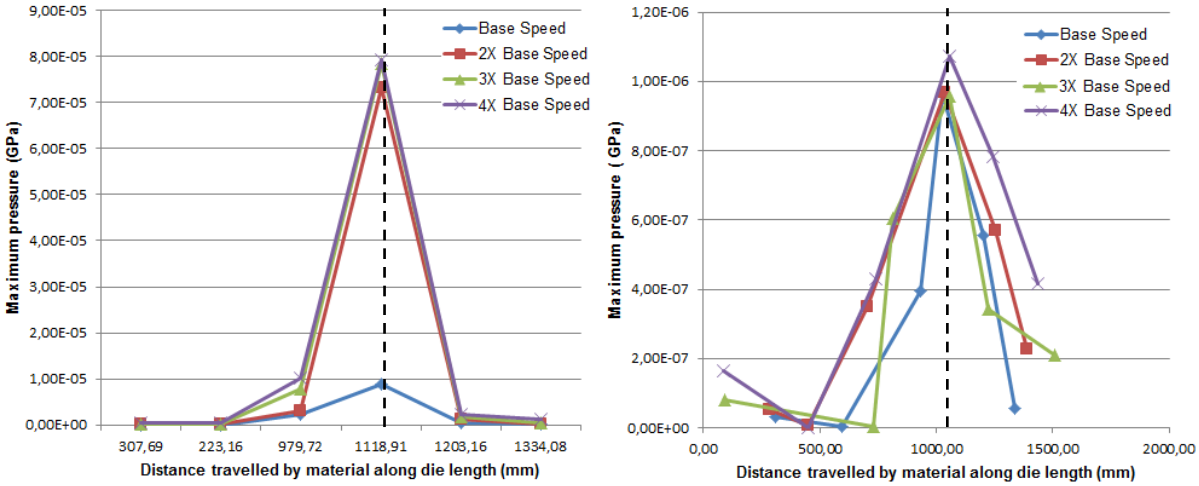


*Fig.41: Maximum pressure in the 6 lower (left) and 6 upper (right) dies vs. distance travelled by material along the die length*

The average pressure on the input material as it moves through the entire tooling is another important factor in the pultrusion process. The compactness of fibers and thermoplastic polymer and the overall quality of consolidation depends upon the pressure as the material moves through the die segments. As described in the pressure model described by Haffner et.al [4] the pressure distribution along the die length presented shows that the pressure increases along the tapered die length. This plot is shown in Figure 42 for the current simulation model for the minimum material model and base pulling speed and shows a similar trend to that in the study performed by Haffner et. al. [4]. This profile is achieved through the definition of a DBFSI keyword card in the database between the ALE fluid part and entire tooling die segment defined as a part set. Overall, it can be observed from the plots and figures that as the speed increases; the pressure on material also increases. The results obtained from this simulation model in general are in line with the study carried out by Kim et. al. [5].

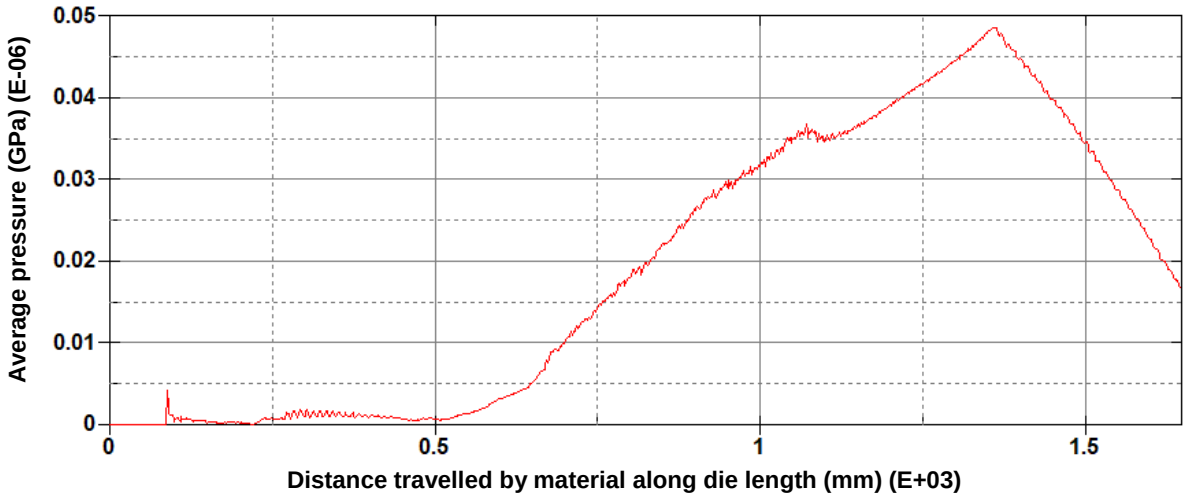


*Fig.42: DBFSI of average pressure on ALE Fluid vs. material travel along the die*

## 5 Conclusions and future scope

This study presented the potential applications of an LS-DYNA ALE/FSI model in order to simulate the thermoplastic pultrusion process. The model is based on real-world input data provided by LG Technology Center Europe and LG Hausys South Korea. A non-continuous FEA model was developed, in which a finite length of three preheated GF/PA6 unidirectional prepreg sheets are passed through the various stages of a pultrusion die. The input material itself was modelled using the coupled combination of an ALE fluid (representing the PA6 polymer) and beam elements (representing the glass fiber rovings). The development of the simulation model was an extensive process involving a large number of keywords used to define the necessary material properties, boundary conditions and in particular the contact and coupling definitions. Various output databases were also setup in order to allow the useful interpretation of the results. The matured simulations consisted of two base speed (0.2 mm/min) pultrusion models with two different quantities of input material which could then be run at different pultrusion pulling speeds. The two base models were termed the “minimum” and “maximum” material input models whereby the minimum material input quantity represented a little more than the exact volume of input material needed to form the desired tube geometry. The maximum material input quantity on the other hand considered double the material volume required to form the 20 mm outer diameter 3 mm thick hollow tube.

For both basis models, the temperature and pressure profiles were obtained and also analyzed at four different pulling speeds. For the minimum material input model these were 2x, 4x and 6x the base speed of 0.2 mm/min and for the maximum material input model 2x, 3x and 4x the base speed of 0.2 mm/min. From the figures and plots generated, it can be concluded that the developed simulation model closely represents the real-world thermoplastic pultrusion process. The effect of pulling speed on the temperature of the material (given the fixed heating conditions on the tooling) was further elaborated by investigating the overall temperature distribution within the material at various stages of the die at each speed. Nodal plots of individual points within the material’s cross-section with respect to the die length were also created. Moreover, the average pressure on the input material due to the different die segments was described for each die segment at different speeds. A comparison of the maximum pressure as well as where this occurs was then concluded for both the minimum and maximum material input models. In addition, it was shown that in the highest pressures do indeed occur in the latter end of the 3rd hot die and the 4th hot die with the highest pressure occurring on the lower hot die as the material enters the first cooling die. The maximum pressure experienced on the upper hot die occurs earlier and is almost 4 times lower. A more gradual temperature transition is therefore suggested on the lower die as the material enters the first cold die. Overall, the temperature and pressure profiles as well as the effect of pulling speed on average pressure and temperatures are all in accordance with studies found in the literature.

During the model development process, three potential material models were identified. However, due to the unavailability of both process and material characterization data it was difficult to use the more complicated models and the simplest of the three (**`*MAT_ELASTIC_PLASTIC_THERMAL`**) was

therefore used in the study here. For ALE simulations, only a limited number of material models are available and not all of these are validated. As mentioned before, a thorough input material characterization and process validation using temperature and pressure sensors mounted on the actual pultrusion equipment needs to be carried out so that a more advanced model can be built.

The development of the non-continuous pultrusion model can be further extended by focusing on the correct interaction between the ALE fluid and the reinforcement fibers/rovings. Fiber tension and maximum tensile stress can be also be evaluated if the fiber to fluid interaction is modeled correctly. With this further development, a study of the pulling force resistance with respect to the pulling speed could also be carried out. Meshless coupled SPH-DEM methods could be also used to model the pultrusion process. Here the SPH particles would be used to represent the polymer while the DEM particles the continuous fibers. Coupling mechanisms for the two already exists in LS-DYNA.

The development of a thermoplastic pultrusion process simulation model has been initiated with the goal of understanding the mechanics of the process. Detailed knowledge regarding the pressure and temperature in different parts of the tooling for different pulling speeds can surely help to optimize the design of new and existing pultrusion lines. Regardless of the unavailability of process and material characterization data it has been shown that the ALE/FSI functionalities in LS-DYNA can be used to investigate the thermoplastic pultrusion process in high detail. A further developed simulation model has enormous potential to enhance the optimization of this manufacturing process further.

## 6 Acknowledgments

The authors would like to thank LG Hausys for their help and support during the course of this project. Our sincere thanks goes to Mr. Hongrok Shin (LG Hausys South Korea) and Dr.-Ing. Jens Dörner (LG Technology Center Europe) in particular for providing the necessary information regarding the pultrusion line in order to allow the setup of a realistic FEA simulation model.

## 7 Literature

[1] Novo, P. J., Silva, J. F., Nunes, J. P., & Marques, A. T.: “Pultrusion of fibre reinforced thermoplastic pre-impregnated materials”, Composites Part B, 2016, 328-339.
[2] Safonov, A. A., Carlone, P., & Akhatov, I.: “Mathematical simulation of pultrusion processes: A review. Composite Structures”, 2018, 184:153-177.
[3] Åström , B. T., & Pipes, R. B.: “A Modelling approach to thermoplastic pultrusion. I: Formulation of models”, Polymer Composites, 1993a, 14.3:173-183.
[4] Haffner, S. M., Friedrich, K., Hogg, P. J., & Busfield, J. C.: “Finite-element-assisted modelling of a thermoplastic pultrusion process for powder-Impregnated yarn”, Composite Science and Technology, 1998, 58: 1371-1380.
[5] Kim, D. H., Lee, W. I., & Friedrich, K.: “A model for a thermoplastic pultrusion process using commingled yarns” Composite Science And Technology, 2001, 61: 1065-1077.
[6] Lee, W. I., Springer, G. S., & Smith, F. N.: “Pultrusion of thermoplastics - A model”, Journal of Composite Materials, 1991, 25:1632-1652.
[7] Donea, J., Heuerta, A., Ponthot, J., & Rodriguez-Ferran, A.: “Arbitrary Lagrangian–Eulerian Methods. In E. Stein, R. Borst, & T. Hughes, Encyclopedia of Computational Mechanics. John Wiley & Sons, 2004.
[8] Souli, M., & Olovson, L.: “Fluid-Structure Interaction in LS DYNA: Industrial Applications”, 4th European LS-DYNA Users Conference. Ulm, Germany, 2003.
[9] Kerbiriou, V., & Friedrich, K.: “Pultrusion of thermoplastic composites-process optimization and mathematical modeling”, Journal of Thermoplastic Composite Materials, 1999, 12.2: 96 - 120.
[10] Tanaka, Y., Torun, A. R., Lebel, L. L., Ohtani, A., & Nakai, A.: “Development of pultrusion system for continuous fiber reinforced thermoplastic composite tube with braiding technique. The 10th International Conference on Flow Processes in Composite Materials, 2010, Ascona, Switzerland.
[11] Åström, B. T., & Pipes, R. B.: “A modelling approach to thermoplastic pultrusion. II: Verification of models”, Polymer Composites, 1993b, 14.3: 184-194.